

Poincaré Inequality for a Mesh-dependent 2-norm on Piecewise Linear Surfaces with Boundary

SHAWN W. WALKER[†]
Department of Mathematics
Louisiana State University
Baton Rouge, LA 70803

[Received on 10 June 2021]

We establish several useful estimates for a non-conforming 2-norm posed on piecewise linear surface triangulations with boundary, with the main result being a Poincaré inequality. We also obtain equivalence of the non-conforming 2-norm posed on the true surface with the norm posed on a piecewise linear approximation. Moreover, we allow for free boundary conditions. The true surface is assumed to be $C^{2,1}$ when free conditions are present; otherwise, C^2 is sufficient. The framework uses tools from differential geometry and the closest point map (see Dziuk (1988)) for approximating the full surface Hessian operator. We also present a novel way of applying the closest point map when dealing with surfaces with boundary. Connections with surface finite element methods for fourth order problems are also noted.

Keywords: surface Hessian ; surfaces with boundary ; mesh-dependent norms ; non-conforming method; surface finite elements.

1. Introduction

The main goal of this paper is to derive a Poincaré inequality for a mesh dependent H^2 norm on piecewise linear surfaces with boundary whether or not free boundary conditions are present. The primary results here are Theorems 4.2 and 4.3, which provide crucial estimates for analyzing finite element methods (FEMs) for fourth order problems on surfaces, e.g. the FEM in Walker (2020) for the surface Kirchhoff plate problem. Many scientific and engineering problems involve elliptic partial differential equations (PDEs) on surfaces, e.g. surface tension Barrett *et al.* (2015); Gerbeau & Lelièvre (2009); Walker *et al.* (2009), surface diffusion Bänsch *et al.* (2005); Smereka (2003), solidification Barrett *et al.* (2010); Davis & Walker (2015, 2017), vesicles Du *et al.* (2005, 2004); Zhong-can & Helfrich (1989); Dziuk (2008); Bonito *et al.* (2010); Barrett *et al.* (2016), and other types of diffusive processes Elliott & Ranner (2015); Elliott & Stinner (2010); Elliott *et al.* (2012). Poincaré inequalities are a necessary tool in analyzing almost any elliptic PDE.

In particular, fourth order elliptic operators appear in some of these applications, e.g. vesicles Bonito *et al.* (2011); Elliott & Stinner (2010) and the surface Cahn-Hilliard equation Elliott & Ranner (2015). It is well-known that fourth order elliptic equations present difficulties for finite element methods (FEMs), even on flat domains. The main issues are dealing with the Sobolev space H^2 and correctly capturing fourth order type boundary conditions. In many instances, a non-conforming approach is preferred for these problems because they avoid C^1 elements, e.g. the Hellan-Herrmann-Johnson method Brezzi & Raviart (1976); Comodi (1989); Blum & Rannacher (1990); Arnold & Walker (2020). Moreover, the

[†]Corresponding author. Email: walker@math.lsu.edu

numerical approximation of fourth order elliptic *surface* PDEs is not as well established as for second order problems Deckelnick *et al.* (2005); Dziuk (1988); Dziuk & Elliott (2013), much less for non-conforming approximations on non-conforming domains (e.g. piecewise linear surfaces). A particularly relevant reference is Larsson & Larson (2017), in which they solve the surface biharmonic problem on a piecewise linear approximation of a *closed* surface using a discontinuous Galerkin (dG) approach.

1.1 Main Contributions

The main motivation of this paper is to better understand the surface Hessian operator on surface triangulations. In particular, we obtain estimates involving a non-conforming surface Hessian operator (i.e. a broken Hessian) on piecewise linear surface triangulations. These estimates are crucial for building effective non-conforming finite element spaces for elliptic problems (posed on surfaces) that require the Sobolev space H^2 . For example, see the FEM in Walker (2020) for the Kirchhoff plate problem posed on a surface.

We establish several useful estimates for a non-conforming H^2 norm (see (2.7)) posed on piecewise linear surface triangulations *with boundary*. The main result is a Poincaré inequality in Theorem 4.2. As a byproduct, we obtain equivalence of the non-conforming H^2 norm posed on the true surface with the norm posed on a piecewise linear approximation (see Theorem 4.3). In addition, we allow for *free boundary conditions*. These results are directly used in Walker (2020).

Our analysis assumes the surface is described by charts that exactly capture its *boundary*. The approximate surface is built by interpolating these charts. For smooth, *closed*, embedded surfaces, one can use the closest point map obtained from a signed distance function to create the approximate surfaces Dziuk (1988); Demlow & Dziuk (2007); Demlow (2009); this method is very convenient for the analysis. However, it is not so convenient for approximating a surface with boundary. Thus, we combine the chart approach with the signed distance function approach to obtain our results.

Furthermore, our analysis deals directly with the (covariant) surface Hessian, in a non-conforming way, which allows for a variety of boundary conditions to be imposed, such as clamped, simply-supported, and free. In fact, the mesh dependent 2-norm equivalence between the piecewise linear surface and the true surface (see (4.15)) holds even if uniform free boundary conditions are used. This is not a trivial result due to the presence of Killing fields (see Section 2.2.2). We also get L^∞ estimates for the mesh dependent 2-norm, i.e. the mesh dependent H^2 space can handle “point conditions.” Lastly, our results hold for continuous Lagrange finite element spaces on surfaces (see Remark 4.2).

1.2 Outline

Section 2 gives the precise surface assumptions, sets up the differential geometry framework, defines the continuous mesh dependent H^2 space, and presents some useful inequalities on the true domain. In Section 3, we describe how the surface is approximated with a piecewise linear triangulation using either the parametric approach or the closest point map. More specifically, we show how to apply the closest point map to surfaces with boundary (see Proposition 3.2); in Burman *et al.* (2019), they also consider surfaces with boundary. We also derive a transformation formula (3.12) for mapping the surface Hessian from a curved triangle in the true (given) surface to a flat triangle in the piecewise linear triangulation. Section 4 gives the main results of the paper, i.e. L^∞ and trace estimates, the Poincaré inequality in (4.5), and the equivalence of norms (see Theorem 4.3), and we close with some remarks in Section 5. Appendix A gives a review of essential differential geometry concepts used in this paper.

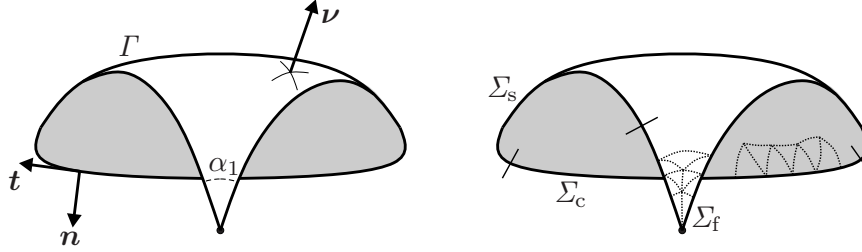


FIG. 1. Illustration of the true (given) surface Γ in \mathbb{R}^3 . The boundary $\Sigma \equiv \partial\Gamma$ decomposes as $\Sigma = \overline{\Sigma_c} \cup \overline{\Sigma_s} \cup \overline{\Sigma_f}$ and has a finite number of corners with interior angles α_i (only one angle is shown); the corners may (or may not) lie at the intersection of two boundary components. The boundary Σ has (outer) conormal vector, \mathbf{n} , and oriented unit tangent vector, \mathbf{t} . The oriented normal vector of Γ is \mathbf{v} . Part of the exact, curved surface triangulation \mathcal{T}_h is shown with dotted curves.

2. Preliminaries

2.1 Domain Assumptions

Let Γ be a connected, 2-dimensional manifold, embedded in \mathbb{R}^3 , with continuous, piecewise smooth boundary $\partial\Gamma =: \Sigma$. In some cases, the boundary may be empty, giving a closed manifold. In particular, Γ is taken to be C^2 and Σ is assumed piecewise C^2 with a finite number of corners, with interior angle $\alpha_i \in (0, 2\pi]$ of the i th corner measured with respect to the Euclidean metric in \mathbb{R}^3 (see Figure 1). In particular, Σ is globally continuous and parameterized by a piecewise curve, i.e., $\Sigma = \bigcup_{p \in \mathcal{V}_\Sigma} p \cup \bigcup_{\zeta \in \mathcal{C}_\Sigma} \zeta$, where \mathcal{V}_Σ is the set of corner vertices and \mathcal{C}_Σ is the set of (open) C^2 curves that make up Σ . Furthermore, as a technical convenience, we assume that Γ is a sub-manifold of Γ^* with $\overline{\Gamma} \subset \subset \Gamma^*$ (see Section 3.3).

In addition, we assume $\Sigma = \overline{\Sigma_c} \cup \overline{\Sigma_s} \cup \overline{\Sigma_f}$ partitions into three mutually disjoint one dimensional components Σ_c (clamped), Σ_s (simply supported), and Σ_f (free). Any of the components can be empty, but if $|\Sigma_f| > 0$, then we also assume that Γ is at least $C^{2,1}$. Each open curve $\zeta \in \mathcal{C}_\Sigma$ belongs to only one of the sets Σ_c , Σ_s , or Σ_f and each curve is maximal such that two distinct curves contained in the same component do not meet at an angle of π . Furthermore, we have the set of corner vertices contained in Σ_f : $\mathcal{V}_{\Sigma_f} = \{p \in \mathcal{V}_\Sigma \mid p = \overline{\zeta_{p^+}} \cap \overline{\zeta_{p^-}}, \text{ where } \zeta_{p^+}, \zeta_{p^-} \subset \Sigma_f, \zeta_{p^+} \neq \zeta_{p^-}\}$.

REMARK 2.1 The choice of nomenclature for partitioning the boundary (i.e. clamped, simply supported, and free) is motivated by bending plate problems. For instance, “linearizing” a geometrically non-linear bending problem yields a plate-like bending problem posed on a fixed surface. One application of the results in this paper is for numerically solving a (fourth order elliptic) plate problem posed on a surface, e.g. Walker (2020).

2.2 Intrinsic Differential Geometry

The notation of intrinsic differential geometry enables a clear characterization of the null space of the surface Hessian operator (Section 2.2.2). It is also convenient for computing tangential differential operators of any order (see Remark 2.3). Thus, the arguments in this section use tensor notation with

special attention paid to upper and lower indices. For instance, using Greek letters, the α -th component of a vector (co-vector) v is denoted as v^α (v_α). Sometimes we write v^a (v_a) to emphasize whether v is a vector or co-vector, where a is a non-numerical label. When $\partial\Gamma \neq \emptyset$, its outer conormal vector has components n_α , while t^α denotes the components of any tangent vector of $\partial\Gamma$. See Section A for a review of tensor notation and differential geometry.

2.2.1 Sobolev Spaces on Manifolds. We write $|v^c|$ and $|v_c|$ to be the “length” with respect to the metric, i.e. $|v^c|^2 = v^\alpha g_{\alpha\beta} v^\beta$ and $|v_c|^2 = v_\alpha g^{\alpha\beta} v_\beta$, where $g_{\alpha\beta}$ is the metric tensor and $g^{\alpha\beta}$ is the inverse metric. In particular, for covariant derivatives, we have

$$|\nabla_c w|^2 = g^{\alpha\beta} \nabla_\alpha w \nabla_\beta w, \quad |\nabla_a \nabla_c w|^2 = g^{\alpha\beta} g^{\gamma\rho} \nabla_\alpha \nabla_\gamma w \nabla_\beta \nabla_\rho w. \quad (2.1)$$

We use standard definitions for Sobolev spaces on manifolds (see Hebey (1996)), i.e. the Sobolev space $W^{k,p}(\Gamma)$ is the completion of $C^\infty(\Gamma)$ with respect to the norm $\|w\|_{W^{k,p}(\Gamma)}^p = \sum_{j=0}^k \int_\Gamma |\nabla_{a_1} \cdots \nabla_{a_j} w|^p dS(g)$, where there are j covariant derivatives in the integrand, and g denotes the determinant of the metric tensor (see Section A). When $p = 2$, the inner product on $W^{k,2}(\Gamma) \equiv H^k(\Gamma)$ is given by

$$(w, v)_{H^k(\Gamma)} := \sum_{j=0}^k \int_\Gamma g^{\alpha_1\beta_1} \cdots g^{\alpha_j\beta_j} (\nabla_{\alpha_1} \cdots \nabla_{\alpha_j} w) (\nabla_{\beta_1} \cdots \nabla_{\beta_j} v) dS(g). \quad (2.2)$$

From (Hebey, 1996, Prop. 2.3), if Γ is compact, then $W^{k,2}(\Gamma)$ does not depend on the Riemannian metric g_{ab} ; the same holds for a bounded C^k manifold with piecewise C^k boundary. We denote by $\dot{H}^k(\Gamma) \subset H^k(\Gamma)$ the Sobolev space with vanishing boundary conditions up to degree $k - 1$. We will have special use of the following subspace of $H^2(\Gamma)$

$$\mathcal{Y}(\Gamma) := \{w \in H^2(\Gamma) \mid w = 0, \text{ on } \Sigma_c \cup \Sigma_s, n^\alpha \nabla_\alpha w = 0, \text{ on } \Sigma_c\}, \quad (2.3)$$

i.e. with clamped and simply-supported boundary conditions.

2.2.2 Null-space of the Hessian. We say a covector field v_α on Γ is a *Killing field* if $\nabla_\alpha v_\beta + \nabla_\beta v_\alpha = 0$, for all $1 \leq \alpha, \beta \leq d$ (Eisenhart, 1926, eqn. (70.2)), (Petersen, 2006, Prop. 27). In addition, the number of independent Killing fields on Γ does not exceed $d(d+1)/2$, where d is the topological dimension of the manifold (Petersen, 2006, Thm. 35). Next, let $\mathcal{Z}(\Gamma) := \{w \in \mathcal{Y}(\Gamma) \mid \nabla_\alpha \nabla_\beta w = 0, \forall 1 \leq \alpha, \beta \leq d\}$ be the nullspace of the covariant Hessian operator $\nabla_\alpha \nabla_\beta (\cdot)$ on Γ . Then, $v_\alpha := \nabla_\alpha w$ is a Killing field for any $w \in \mathcal{Z}(\Gamma)$, because the Hessian is symmetric. So $\dim \mathcal{Z}(\Gamma) \leq 1 + d(d+1)/2$ since $\mathcal{Z}(\Gamma)$ also contains constants. If $\partial\Gamma \equiv \emptyset$, then $\mathcal{Z}(\Gamma)$ only contains constants. Moreover, if $|\Sigma_c| > 0$ or $\partial\Gamma \equiv \Sigma_s$, then $\mathcal{Z}(\Gamma)$ is trivial.

Otherwise, when $d = 2$ or 3 , the maximum dimension of $\mathcal{Z}(\Gamma)$ is $d + 1$, which we now show. Let $\{\mathbf{p}_j\}_{j=1}^{d+1}$ be the vertices of a d -dimensional “simplex” contained in Γ where each pair of vertices is connected by a unique shortest geodesic path. Thus, there are d geodesics emanating from each vertex \mathbf{p}_j , and we assume that the simplex is chosen so that the tangent vectors of the geodesics, at \mathbf{p}_j , span the tangent space $T_{\mathbf{p}_j}(\Gamma)$ for all $1 \leq j \leq d + 1$.

Owing to the continuous embedding $H^2(\Gamma) \hookrightarrow C^0(\bar{\Gamma})$, point evaluation is well-defined. Thus, let $w \in \mathcal{Z}(\Gamma)$ be such that $w(\mathbf{p}_j) = 0$, for $1 \leq j \leq d + 1$, and set $v_\alpha := \nabla_\alpha w$. Since $\nabla_b v_a$ vanishes, if v_a vanishes at a point, then v_a must vanish everywhere (do Carmo, 1992, Ch. 3, exer. 6). Thus, if v_a does not vanish at the vertex \mathbf{p}_j , there is another vertex \mathbf{p}_k (with $k \neq j$), with geodesic path γ connecting them

whose tangent vector q^α satisfies $v_\alpha q^\alpha = c \neq 0$ at \mathbf{p}_j . In addition, $v_\alpha q^\alpha = c$ along the entire geodesic path Υ (do Carmo, 1992, Ch. 5, Prop. 3.6 and exer. 8). Since $0 = w(\mathbf{p}_k) - w(\mathbf{p}_j) = \int_\Upsilon v_\alpha q^\alpha ds = c|\Upsilon|$, we have that v_α must vanish, and so w must also vanish. Therefore, $w(\mathbf{p}_j) = 0$, for $1 \leq j \leq d$, are linearly independent conditions, i.e. the maximum dimension of $\mathcal{Z}(\Gamma)$ is $d + 1$.

REMARK 2.2 Generic manifolds, with non-constant Gauss curvature, do not have Killing fields. Ergo, even if $\partial\Gamma \equiv \Sigma_f$, $\mathcal{Z}(\Gamma)$ may only contain constants. On the other hand, consider the closed 2-sphere. It has 3 Killing fields corresponding to 3 independent rotations of the sphere, but none of them come from differentiating a scalar w (so $\mathcal{Z}(\Gamma)$ only contains constants).

Next, consider a small spherical cap with boundary (and free boundary conditions). Two of the Killing fields can be written as a gradient, but the third one is a rotation about a point in the surface so does not correspond to the gradient of a scalar (see (do Carmo, 1992, Ch. 4, exer. 3.)). In this case, $\mathcal{Z}(\Gamma)$ is spanned by three basis functions, i.e. two non-constant functions whose gradients are Killing fields and the unit constant function.

2.3 Extrinsic Differential Geometry

We use the embedding space and make explicit use of the parametrization of the manifold (i.e. its atlas of charts). This is often more practical for computations, especially when the manifold is defined by an explicit parametrization. Throughout the rest of the paper, we assume $d = 2$ (intrinsic dimension) and $n = 3$ (embedding dimension). Extrinsic vectors and tensors are denoted with bold-face (see Figure 1). Moreover, the $H^1(\Gamma)$ inner product on Γ can be written (c.f. (2.2)):

$$(w, v)_{H^1(\Gamma)} := \int_\Gamma wv + \nabla_\Gamma w \cdot \nabla_\Gamma v dS, \quad (w, v)_{H^2(\Gamma)} := (w, v)_{H^1(\Gamma)} + \int_\Gamma \nabla_\Gamma \nabla_\Gamma w : \nabla_\Gamma \nabla_\Gamma v dS, \quad (2.4)$$

where $\nabla_\Gamma v$ is the surface gradient of v in (A.6) and $\nabla_\Gamma \nabla_\Gamma v$ is the surface Hessian in (A.7); later, we consider a piecewise (broken) Hessian (see (2.6) and (2.7)). See Section A.2 for details of the notation and differential operator definitions.

REMARK 2.3 A popular way to define the surface gradient $\nabla_\Gamma v$ uses the ambient space and projects the standard Euclidean gradient onto the tangent plane of the surface (see Delfour & Zolésio (2011); Demlow (2009); Dziuk & Elliott (2013); Walker (2015); Larsson & Larson (2017); Burman *et al.* (2019), and many others). However, we stress that $\nabla_\Gamma \nabla_\Gamma v$ is *not* the surface gradient ∇_Γ applied to each component of $\nabla_\Gamma v$. Computing in this way would yield a matrix that is not symmetric and is not tangential.

Therefore, we opt for the standard differential geometry approach that uses charts and the induced metric tensor. In this framework, differential operators (e.g. covariant derivatives), of any order, are necessarily tangential. In addition, the covariant Hessian is a symmetric tensor. One obtains the extrinsic operator, e.g. $\nabla_\Gamma \nabla_\Gamma v$, by contracting the covariant operator with the contravariant basis vectors of the tangent space; this preserves tangential-ness of the operator and symmetry. An important contribution of this paper is to demonstrate the effectiveness of the intrinsic approach for analyzing and computing with surface finite elements. See Appendix A for more details.

2.3.1 Skeleton Mesh. We partition Γ with a mesh $\mathcal{T}_h = \{T\}$ of triangles such that $\Gamma = \bigcup_{T \in \mathcal{T}_h} T$, where $h_T := \text{diam}(T)$ and $h := \max_T h_T$, and assume throughout that the mesh is quasi-uniform and shape regular. We also assume the corners of the domain are captured by vertices of the mesh. Note that these triangles are, in general, curved. See Figure 1.

Next, we have the *skeleton* of the mesh, i.e. the set of mesh edges $\mathcal{E}_h := \partial \mathcal{T}_h$, which may be curved. Let $\mathcal{E}_{\partial,h} \subset \mathcal{E}_h$ denote the subset of edges that are contained in the boundary Σ and respect the boundary condition partition of Σ . The internal edges are given by $\mathcal{E}_{0,h} := \mathcal{E}_h \setminus \mathcal{E}_{\partial,h}$.

2.3.2 Continuous Mesh-dependent Spaces. The main difficulty in building finite element subspaces of $H^2(\Gamma)$ is that C^1 elements are required for a conforming discretization. This is especially difficult in the case of a surface, e.g. one would need a surface version of the Argyris element Brenner & Scott (2008). Instead, we introduce a mesh-dependent version of $H^2(\Gamma)$ (see Brezzi & Raviart (1976); Babuška *et al.* (1980); Arnold, D. N. & Brezzi, F. (1985); Blum & Rannacher (1990); Arnold & Walker (2020)).

The following spaces are infinite dimensional, but “mesh dependent.” Thus, we use standard dG notation for writing inner products and norms over the triangulation, e.g. $(f, g)_{\mathcal{T}_h} := \sum_{T \in \mathcal{T}_h} (f, g)_T$, $\|f\|_{L^p(\mathcal{T}_h)}^p := \sum_{T \in \mathcal{T}_h} \|f\|_{L^p(T)}^p$, etc. The following scaling/trace estimate is used judiciously (Agmon, 1965, Thm 3.10):

$$\|v\|_{L^2(\partial T)}^2 \leq C \left(h^{-1} \|v\|_{L^2(T)}^2 + h \|\nabla_{\Gamma} v\|_{L^2(T)}^2 \right), \quad \forall v \in H^1(T), T \in \mathcal{T}_h. \quad (2.5)$$

We follow Babuška *et al.* (1980) in defining infinite dimensional, but mesh dependent spaces and norms. A mesh-dependent version of $H^2(\Gamma)$ is given by

$$H_h^2(\Gamma) := \{v \in H^1(\Gamma) \mid v|_T \in H^2(T), \text{ for } T \in \mathcal{T}_h\}, \quad (2.6)$$

with the following semi-norm

$$\|v\|_{2,h}^2 := \|\nabla_{\Gamma} \nabla_{\Gamma} v\|_{L^2(\mathcal{T}_h)}^2 + h^{-1} \|[\mathbf{n} \cdot \nabla_{\Gamma} v]\|_{L^2(\mathcal{E}_{0,h})}^2 + h^{-1} \|[\mathbf{n} \cdot \nabla_{\Gamma} v]\|_{L^2(\Sigma_c)}^2, \quad (2.7)$$

where $[\eta]$ is the jump in quantity η across mesh edge E . More specifically, if the edge E is shared by two triangles T_1 and T_2 with outward co-normals \mathbf{n}_1 and \mathbf{n}_2 , then $[\mathbf{n} \cdot \nabla_{\Gamma} v]|_E = \mathbf{n}_1 \cdot \nabla_{\Gamma} v|_{T_1 \cap E} + \mathbf{n}_2 \cdot \nabla_{\Gamma} v|_{T_2 \cap E}$. For $E \in \mathcal{E}_{\partial,h}$, with $E \subset \partial T$, we set $[\eta]|_E = \eta|_{T \cap E}$.

Suppose $\{\mathbf{p}_j\}_{j=1}^{d+1} \subset \Gamma$ are chosen as discussed in Section 2.2.2. Set $J = \dim \mathcal{Z}(\Gamma)$ and let $\Xi(f) := \left(\sum_{j=1}^J |f(\mathbf{p}_j)|^2 \right)^{1/2}$ for all $f \in H_h^2(\Gamma)$ if $J > 0$; otherwise, $\Xi(f) \equiv 0$. Next, introduce the following mesh dependent subspace

$$\mathcal{W}_h := \{w \in H_h^2(\Gamma) \mid w = 0 \text{ on } \Sigma_c \cup \Sigma_s, \Xi(w) = 0\} \subset H^1(\Gamma), \quad (2.8)$$

where \mathcal{W}_h is a mesh-dependent version of $\mathcal{Z}(\Gamma)$. The point condition $\Xi(w) = 0$ makes sense because of the continuous embedding $H_h^2(\Gamma) \hookrightarrow C^0(\bar{\Gamma})$ (see (2.9)), and is needed to avoid a non-trivial null space of the Hessian (recall the discussion on Killing fields in Section 2.2.2). Note that the slope condition in (2.3) is not imposed in (2.8), but is “enforced” through the norm (2.7). The space in (2.8) appears in the finite element method discussed in Walker (2020).

2.4 Inequalities on the True Manifold

The proofs of the following propositions utilize standard compactness arguments and convolution on surfaces (see Adams & Fournier (2003); Hebey (1996)). Hence, we only give the proof of Proposition 2.3; the others are similar. Recall that if Γ has a boundary, then we assume $\bar{\Gamma}$ is compactly contained in a larger surface Γ^* .

PROPOSITION 2.1 On the true manifold, Γ , define $\|v\|_{\bullet,h}^2 := \|v\|_{H^1(\Gamma)}^2 + \|\nabla_\Gamma \nabla_\Gamma v\|_{L^2(\mathcal{T}_h)}^2$, for any $v \in H_h^2(\Gamma)$. Then, for all $h > 0$,

$$\|v\|_{L^\infty(\Gamma)} \leq C_{\text{inf}} \|v\|_{\bullet,h}, \quad \forall v \in H_h^2(\Gamma), \quad (2.9)$$

$$\|\nabla_\Gamma v\|_{L^2(\partial\Gamma)} \leq C_{\text{tr}} \left(\|\nabla_\Gamma v\|_{L^2(\Gamma)}^2 + \|\nabla_\Gamma \nabla_\Gamma v\|_{L^2(\mathcal{T}_h)}^2 \right)^{1/2}, \quad \text{for all } v \in H_h^2(\Gamma), \quad (2.10)$$

with constants $C_{\text{inf}}, C_{\text{tr}} > 0$ that depend on Γ and the shape regularity of \mathcal{T}_h , but do *not* depend on h .

Next, we have two Poincaré type inequalities posed on the true manifold Γ .

PROPOSITION 2.2 Recall the definition of $\|\cdot\|_{2,h}$ in (2.7). Then, $\|\cdot\|_{2,h}$ is a norm on \mathcal{W}_h in (2.8). Moreover, define $\|v\|_h^2 := \|v\|_{2,h}^2 + \|v\|_{L^2(\Sigma_c \cup \Sigma_s)}^2 + \mathfrak{E}^2(v)$, for any $v \in H_h^2(\Gamma)$. Then, there is a constant $C_* > 0$, depending only on Γ and the shape regularity of \mathcal{T}_h (but independent of h), such that

$$\|v\|_{L^2(\Gamma)} \leq C_* \left(\|\nabla_\Gamma v\|_{L^2(\Gamma)}^2 + \|v\|_h^2 \right)^{1/2}, \quad \text{for all } v \in H_h^2(\Gamma). \quad (2.11)$$

PROPOSITION 2.3 Adopt the hypothesis of Proposition 2.2. Then there is a constant $C_P > 0$, depending only on Γ and the shape regularity of \mathcal{T}_h (but independent of h), such that

$$\|\nabla_\Gamma v\|_{L^2(\Gamma)} \leq C_P \|v\|_h, \quad \text{for all } v \in H_h^2(\Gamma). \quad (2.12)$$

Proof. From the discussion in Section 2.2.2, it is clear that (for a fixed h), one can use a standard compactness argument to show that $\|\nabla_\Gamma v\|_{L^2(\Gamma)} \leq C_1 \|v\|_h$, for all $v \in H_h^2(\Gamma)$, where $C_1 = C_1(h) \geq 1$ may depend on h . Suppose that (2.12) is false; then, there exists a sequence $\{w_h\}_{h>0}$, with $w_h \in H_h^2(\Gamma)$, such that $\|\nabla_\Gamma w_h\|_{L^2(\Gamma)} > \frac{1}{\delta(h)} \|w_h\|_h$, where $\delta(h) \rightarrow 0$ as $h \rightarrow 0$. Define

$$u_h := \frac{w_h}{\|\nabla_\Gamma w_h\|_{L^2(\Gamma)}} \Rightarrow \|\nabla_\Gamma u_h\|_{L^2(\Gamma)} = 1, \quad \forall h, \quad \text{and} \quad \|u_h\|_h < \delta(h), \quad \forall h. \quad (2.13)$$

In addition, we have a bound on the $L^2(\Gamma)$ norm via (2.11), i.e. $\|u_h\|_{L^2(\Gamma)} \leq C$ uniformly for all h . Next, for each fixed h , given $\varepsilon > 0$, construct $u_{h,\varepsilon} \in H^2(\Gamma)$ such that

$$\begin{aligned} |u_h - u_{h,\varepsilon}|_{H^2(\mathcal{T}_h)} &\leq \varepsilon, & \|u_h - u_{h,\varepsilon}\|_{H^1(\Gamma)} &\leq \varepsilon, \\ h^{-1} \|\mathbf{n} \cdot \nabla_\Gamma (u_h - u_{h,\varepsilon})\|_{L^2(\Sigma_c)} &\leq \varepsilon, & |u_h(\mathbf{p}_i) - u_{h,\varepsilon}(\mathbf{p}_i)| &\leq \varepsilon, \end{aligned} \quad (2.14)$$

for $i = 1, \dots, J$ (e.g. use convolution on surfaces; see Adams & Fournier (2003); Hebey (1996)); the last relation is possible because $u_h \in C^0(\bar{\Gamma})$ for all h . The normal derivative bound follows by a trace inequality on elements attached to Σ_c (and taking a sufficiently tight convolution).

Now, define

$$\tilde{u}_h := u_{h,\varepsilon_h} \in H^2(\Gamma), \quad \text{where} \quad \varepsilon_h = \delta(h). \quad (2.15)$$

Then, by combining the above results, $\|\tilde{u}_h\|_{H^2(\Gamma)} \leq C$, uniformly for all h , i.e.

$$\begin{aligned} \|\tilde{u}_h\|_{H^2(\Gamma)} &\leq \|\tilde{u}_h\|_{L^2(\Gamma)} + \|\nabla_\Gamma \tilde{u}_h\|_{L^2(\Gamma)} + |\tilde{u}_h|_{H^2(\mathcal{T}_h)} \\ &\leq 3\varepsilon_h + \|u_h\|_{L^2(\Gamma)} + \|\nabla_\Gamma u_h\|_{L^2(\Gamma)} + |u_h|_{H^2(\mathcal{T}_h)} \\ &\leq 3\delta(h) + C + 1 + \|u_h\|_h < 4\delta(h) + C + 1. \end{aligned} \quad (2.16)$$

Ergo, \tilde{u}_h converges weakly in $H^2(\Gamma)$, and $\tilde{u}_h \rightarrow \tilde{u}$ strongly in $H^1(\Gamma)$. Moreover,

$$|\tilde{u}_h|_{H^2(\Gamma)} = |\tilde{u}_h|_{H^2(\mathcal{T}_h)} \leq |u_h - \tilde{u}_h|_{H^2(\mathcal{T}_h)} + \|u_h\|_h \leq \varepsilon_h + \delta(h) = 2\delta(h), \quad (2.17)$$

so $\nabla_\Gamma \nabla_\Gamma \tilde{u}_h \rightarrow 0$ in $L^2(\Gamma)$. By the definition of the weak derivative, and weak convergence, $\nabla_\Gamma \nabla_\Gamma \tilde{u} \equiv 0$, meaning that $\tilde{u}_h \rightarrow \tilde{u}$ strongly in $H^2(\Gamma)$.

By standard trace inequalities, $\tilde{u} = 0$ on $\Sigma_c \cup \Sigma_s$ (because $\|u_h\|_{L^2(\Sigma_c \cup \Sigma_s)} \rightarrow 0$). Moreover, using (2.14), we have that $h^{-1} \|\mathbf{n} \cdot \nabla_\Gamma \tilde{u}_h\|_{L^2(\Sigma_c)} \leq 2\delta(h)$, i.e. $\mathbf{n} \cdot \nabla_\Gamma \tilde{u} = 0$ on Σ_c . Thus, \tilde{u} is in the nullspace $\mathcal{L}(\Gamma)$. In addition, in a similar fashion as above, we can show $\tilde{u}(\mathbf{p}_i) = 0$ for $i = 1, \dots, J$. So, based on the discussion in Section 2.2.2, it must be that $\tilde{u} \equiv 0$.

Therefore, $\tilde{u}_h \rightarrow 0$ in $H^2(\Gamma)$. But recall that $1 = \|\nabla_\Gamma u_h\|_{L^2(\Gamma)}$ for all h , so then

$$1 = \|\nabla_\Gamma u_h\|_{L^2(\Gamma)} \leq \|\nabla_\Gamma (u_h - \tilde{u}_h)\|_{L^2(\Gamma)} + \|\nabla_\Gamma \tilde{u}_h\|_{L^2(\Gamma)} \rightarrow 0, \quad (2.18)$$

because $\|\nabla_\Gamma (u_h - \tilde{u}_h)\|_{L^2(\Gamma)} \leq \delta(h)$ from (2.14). Obviously, (2.18) is a contradiction, so we have established (2.12). \square

3. Domain Approximation and Mappings

Our main goal is to show that the Poincaré inequality (2.12) still holds when Γ is replaced by a piecewise linear approximation Γ^1 . In particular, given our embedded manifold Γ , with or without boundary, and a piecewise linear triangulation Γ^1 that interpolates Γ at its vertices, we need certain approximation results when mapping flat triangles in Γ^1 to Γ .

Any *closed* C^2 surface may be represented as the zero level set of a signed distance function. This is especially convenient for defining the *closest point map*, which enjoys nice approximation properties (see Demlow & Dziuk (2007); Demlow (2009); Dziuk & Elliott (2013); Dziuk (1988)). However, it is not so convenient for dealing with surfaces with boundary. On the other hand, any C^2 surface may be parametrized by an atlas of charts $\{(U_i, \boldsymbol{\chi}_i)\}$ which captures the boundary exactly. The following sections combine these two approaches to yield new estimates on mapping the full surface Hessian operator from Γ^1 to Γ . In the following, we assume we have access to an atlas of charts $\{(U_i, \boldsymbol{\chi}_i)\}$, where U_i is the reference domain and $\boldsymbol{\chi}_i$ is the corresponding map, that parameterizes Γ , and its boundary, exactly.

3.1 Piecewise Linear Triangulations and the True Domain

Given our embedded manifold Γ , with or without boundary, we assume that a conforming, shape regular, piecewise linear triangulation \mathcal{T}_h^1 of a polyhedral domain Γ^1 that interpolates Γ at its vertices can be generated provided the mesh size is sufficiently small; we refer to Demlow & Dziuk (2007); Demlow (2009); Dziuk & Elliott (2013); Dziuk (1988) for more discussion on these basic issues. Furthermore, we assume the boundary vertices of Γ^1 (namely $\Sigma^1 := \partial\Gamma^1$) lie on the boundary of Γ . Let $\mathcal{T}_{\partial,h}^1$ be the set of triangles with one side on Σ^1 and, for convenience, assume the triangulation satisfies the following property.

Property 1 Each triangle in \mathcal{T}_h^1 has at most two vertices on the boundary and so has at most one edge contained in Σ^1 .

We denote by \mathcal{E}_h^1 the set of edges of the triangulation \mathcal{T}_h^1 , which is partitioned into interior edges $\mathcal{E}_{0,h}^1$ and boundary edges $\mathcal{E}_{\partial,h}^1$. Thus $\Sigma^1 := \bigcup_{E^1 \in \mathcal{E}_{\partial,h}^1} E^1$ is a 1st order approximation of Σ . We also assume

\mathcal{T}_h^1 is homeomorphic to an exact triangulation \mathcal{T}_h of Γ in the following sense. For each $T^1 \in \mathcal{T}_h^1$, there is a chart $(U, \boldsymbol{\chi})$, and a straight-edged triangle $T' \subset U$, such that the following holds.

- (i) $T^1 = (\mathcal{I}_h \boldsymbol{\chi})(T')$, where \mathcal{I}_h is the standard continuous linear, nodal Lagrange interpolation operator with the usual approximation properties.
- (ii) There is a unique $T \in \mathcal{T}_h$ such that $T = \boldsymbol{\chi}(T')$.

With the above considerations, one can generate another atlas of charts $\{(\widehat{T}, \boldsymbol{\chi}_T)\}_{T \in \mathcal{T}_h}$, where for each $T \in \mathcal{T}_h$, $T = \boldsymbol{\chi}_T(\widehat{T})$, where \widehat{T} is the standard reference triangle. Next, for each $T^1 \in \mathcal{T}_h^1$, we define the mapping $\mathbf{F} : \Gamma^1 \rightarrow \Gamma$ through the diffeomorphism $\mathbf{F}_T \equiv \mathbf{F}|_{T^1} := \boldsymbol{\chi}_T \circ (\mathcal{I}_h \boldsymbol{\chi}_T)^{-1}$. The true domain, and its corresponding triangulation, can be viewed as an “infinite order” approximation. Ergo, we adopt the following notations $\Gamma^\infty \equiv \Gamma$, $\mathcal{T}_h^\infty \equiv \mathcal{T}_h$, $\mathbf{F}_T^\infty \equiv \mathbf{F}_T$, etc., which will sometimes be convenient (it is merely a choice of notation).

The main approximation properties for these maps are summarized in the next theorem.

THEOREM 3.1 The map \mathbf{F}_T described above satisfies

$$\begin{aligned} \|\nabla_{T^1}^s(\mathbf{F}_T - \text{id}_{T^1})\|_{L^\infty(T^1)} &\leq Ch^{2-s}, \quad \text{for } s = 0, 1, 2, \\ 1 - Ch &\leq \|[\nabla_{T^1} \mathbf{F}_T]^{-1}\|_{L^\infty(T^1)} \leq 1 + Ch, \quad \|[\nabla_{T^1} \mathbf{F}_T]^{-1} - \mathbf{I}\|_{L^\infty(T^1)} \leq Ch, \end{aligned} \quad (3.1)$$

where all constants depend on the C^2 norm of Γ .

3.2 Element-wise Parametrization

It is useful to consider the map $\mathbf{F}_T : T^1 \rightarrow T$ from Section 3.1 as a parametrization of T in the following sense. Apply a rigid rotation of coordinates \mathbf{x} to \mathbf{x}' so that $T^s \rightarrow T^{s'}$ (for $s = 1$ or ∞) and $T^{1'} \subset \mathbb{R}^2$. In the rotated coordinates, we view \mathbf{F}_T as a function of two variables, so that $(T^{1'}, \mathbf{F}_T')$ is a local chart for T' . Next, let $\mathbf{J}' = [\partial_1 \mathbf{F}_T', \partial_2 \mathbf{F}_T']$ be the 3×2 Jacobian matrix with induced metric $\mathbf{g}' = (\mathbf{J}')^T \mathbf{J}'$. In addition, define the 3×2 matrix $\bar{\mathbf{P}}_*'^T = [\mathbf{a}_1, \mathbf{a}_2]$, where $\{\mathbf{a}_1, \mathbf{a}_2, \mathbf{a}_3\}$ are the canonical basis vectors of \mathbb{R}^3 , $(\bar{\mathbf{P}}_*')^T \bar{\mathbf{P}}_*' = \mathbf{I}_2$, and $\bar{\mathbf{P}}_*'^T (\bar{\mathbf{P}}_*')^T = \bar{\mathbf{P}}' := \mathbf{I}_3 - \bar{\mathbf{v}}' \otimes \bar{\mathbf{v}}'$, where $\bar{\mathbf{v}}' \equiv \mathbf{a}_3$ is the unit normal of $T^{1'}$.

All results derived in the rotated coordinates can be mapped back to the original coordinates. For example, let $\bar{\mathbf{P}}_* = [\mathbf{b}_1, \mathbf{b}_2]$, where $\mathbf{b}_1, \mathbf{b}_2$ are any two orthogonal unit vectors in \mathbb{R}^3 pointing in the plane of T^1 , and note that $\bar{\mathbf{P}}_*^T \bar{\mathbf{P}}_* = \mathbf{I}_2$, and $\bar{\mathbf{P}}_* \bar{\mathbf{P}}_*^T = \bar{\mathbf{P}} := \mathbf{I}_3 - \bar{\mathbf{v}} \otimes \bar{\mathbf{v}}$ (see (A.11)), where $\bar{\mathbf{v}} = \mathbf{b}_1 \times \mathbf{b}_2$ is the unit normal of T^1 . Then, $\mathbf{J} = (\nabla_{T^1} \mathbf{F}_T) \bar{\mathbf{P}}_*$, $\mathbf{g} = \mathbf{J}^T \mathbf{J}$, and by (3.1),

$$|\mathbf{J} - \bar{\mathbf{P}}_*| = O(h), \quad \mathbf{g} = \bar{\mathbf{P}}_*^T \bar{\mathbf{P}}^T \bar{\mathbf{P}} \bar{\mathbf{P}}_* + O(h) = \mathbf{I}_2 + O(h), \quad (3.2)$$

so \mathbf{g} is invertible for h sufficiently small. Note that, in terms of \mathbf{F}_T , the surface gradient (A.6) of $f : T \rightarrow \mathbb{R}$ can be written as $(\nabla_T f) \circ \mathbf{F}_T = (\nabla_{T^1} \bar{f}) \bar{\mathbf{P}}_* \mathbf{g}^{-1} \mathbf{J}^T$, where $\bar{f} := f \circ \mathbf{F}_T$. Moreover, using the parametrization above, in the rotated coordinates the Christoffel symbols (A.1) have a more explicit form: $\Gamma_{\alpha\beta}^\gamma = ((\mathbf{g}')^{-1} (\mathbf{J}')^T \mathbf{a}_i)^\gamma \partial_\alpha \partial_\beta (\mathbf{F}_T' \cdot \mathbf{a}_i)$. Ergo, the surface Hessian (A.7), in the original coordinates, can be written as

$$\begin{aligned} (\nabla_T \nabla_T f) \circ \mathbf{F}_T &= \mathbf{J} \mathbf{g}^{-1} \bar{\mathbf{P}}_*^T [\nabla_{T^1} \nabla_{T^1} \bar{f}] \bar{\mathbf{P}}_* \mathbf{g}^{-1} \mathbf{J}^T \\ &\quad - ((\nabla_{T^1} \bar{f}) \bar{\mathbf{P}}_* \mathbf{g}^{-1} \mathbf{J}^T \mathbf{a}_i) \mathbf{J} \mathbf{g}^{-1} \bar{\mathbf{P}}_*^T [\nabla_{T^1} \nabla_{T^1} (\mathbf{F}_T \cdot \mathbf{a}_i)] \bar{\mathbf{P}}_* \mathbf{g}^{-1} \mathbf{J}^T. \end{aligned} \quad (3.3)$$

3.3 Closest Point Map

The results in this section are crucial to prove the Poincaré inequality (4.5) when Γ has a boundary where part of the boundary imposes free conditions (i.e. $|\Sigma_f| > 0$).

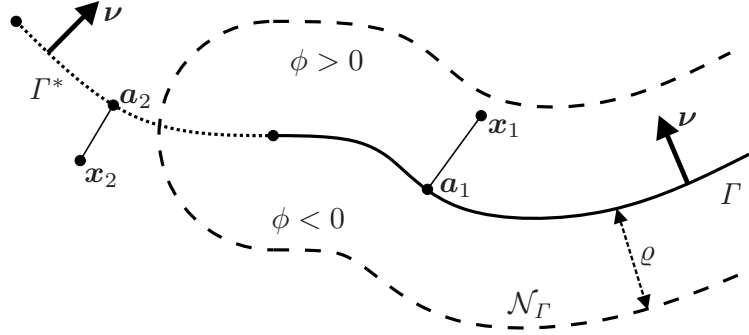


FIG. 2. Diagram of $\bar{\Gamma} \subset \subset \Gamma^*$ and the tubular neighborhood \mathcal{N}_Γ . The solid curve is Γ and the dotted curve is Γ^* ; the dashed curve denotes the boundary of \mathcal{N}_Γ . The closest point map is illustrated by $\text{clp}^*(x_i) = a_i$, for $i = 1, 2$, and is characterized by $\text{clp}^*(\mathbf{x}) \equiv \mathbf{x} - \phi(\mathbf{x})\mathbf{v}^*(\mathbf{x})$, where $\phi(\mathbf{x})$ is a signed distance function for Γ^* that is well-defined in \mathcal{N}_Γ .

Let $\Gamma \subset \mathbb{R}^n$ be a $d = n - 1$ dimensional C^2 embedded manifold, possibly with C^2 boundary $\partial\Gamma$, and let $\text{clp} : \mathbb{R}^n \rightarrow \Gamma$ be the closest point map, i.e. $|\text{clp}(\mathbf{x}) - \mathbf{x}| = \text{dist}(\mathbf{x}, \Gamma)$. Define the “tubular” neighborhood $\mathcal{N}_\Gamma(c) := \{\mathbf{x} \in \mathbb{R}^n \mid \text{dist}(\mathbf{x}, \Gamma) < c\}$, for any positive constant c . If $\partial\Gamma \neq \emptyset$, then we also assume that $\bar{\Gamma} \subset \subset \Gamma^*$, where Γ^* is an extended d dimensional, C^2 manifold, with boundary $\partial\Gamma^*$ and corresponding closest point map $\text{clp}^* : \mathbb{R}^n \rightarrow \Gamma^*$. See Figure 2.

3.3.1 Signed Distance Function. Next, we construct a *signed distance function* for Γ^* . Letting $\mathbf{v}^* : \Gamma^* \rightarrow \mathbb{R}^n$ be the oriented normal of Γ^* , we define $\phi(\mathbf{x}) := \text{sgn}(\nabla \varpi(\mathbf{x}) \cdot (\mathbf{v}^* \circ \text{clp}^*(\mathbf{x})))\varpi(\mathbf{x})$, for all \mathbf{x} in \mathbb{R}^n , where $\varpi(\mathbf{x}) := \text{dist}(\mathbf{x}, \Gamma^*)$ (see Figure 2). Now assume there exists a $\rho > 0$, with $\mathcal{N}_\Gamma(\rho) \equiv \mathcal{N}_\Gamma$, such that $\phi \in C^2(\mathcal{N}_\Gamma)$ and $|\nabla\phi| = 1$ in \mathcal{N}_Γ Gromov (1991), (Delfour & Zolésio, 2011, pg. 75); clearly, ρ depends on Γ (e.g. its curvature) and how far Γ can be extended with Γ^* . Thus, $\Gamma^* \cap \mathcal{N}_\Gamma \equiv \{\mathbf{x} \in \mathcal{N}_\Gamma \mid \phi(\mathbf{x}) = 0\}$, and $\mathbf{v}^*(\mathbf{x}) = (\nabla\phi)^T(\mathbf{x})$ on $\Gamma^* \cap \mathcal{N}_\Gamma$. Indeed, we define the *extended normal vector* by $\mathbf{v}^*(\mathbf{x}) = (\nabla\phi)^T(\mathbf{x})$ for all $\mathbf{x} \in \mathcal{N}_\Gamma$, and the extended tangent space projection by $\mathbf{P}^* = \mathbf{I} - \mathbf{v}^* \otimes \mathbf{v}^*$. Moreover, the following relation holds *uniquely*: $\mathbf{x} = \text{clp}^*(\mathbf{x}) + \phi(\mathbf{x})\mathbf{v}^*(\mathbf{x})$, for all $\mathbf{x} \in \mathcal{N}_\Gamma$. We can *extend* a function u , defined on Γ^* , to \mathcal{N}_Γ via the signed distance function, i.e.

$$u_e(\mathbf{x}) := u \circ \Phi(\mathbf{x}), \quad \forall \mathbf{x} \in \mathcal{N}_\Gamma, \quad \text{where } \Phi(\mathbf{x}) := \text{clp}^*(\mathbf{x}) \equiv \mathbf{x} - \phi(\mathbf{x})\mathbf{v}^*(\mathbf{x}), \quad (3.4)$$

which is known as a constant extension in the normal direction.

REMARK 3.1 In Burman *et al.* (2019), they also consider a surface with boundary. They assume that the given surface is contained in a *closed surface* that has a well-defined closest point map. Thus, mapping to the original surface is done using the map generated from the closed surface. The approach we take here is more general.

For any piecewise linear triangulation \mathcal{T}_h^1 of Γ , whose domain is denoted Γ^1 and contained in \mathcal{N}_Γ , we can “lift” it to a subset of Γ^* using Φ . In other words, define $\check{\mathcal{T}}_h := \{\Phi(T^1) \mid T^1 \in \mathcal{T}_h^1\}$ to be an

“exact” triangulation and set $\check{\Gamma} := \cup_{\check{T} \in \check{\mathcal{T}}_h} \check{T} \subset \Gamma^*$. In addition, from $\check{\mathcal{T}}_h$, we have the following related sets: $\check{\mathcal{T}}_{\partial,h}$, $\check{\mathcal{E}}_{0,h}$, and $\check{\mathcal{E}}_{\partial,h}$ (see Sections 2.3.2, 3.1).

Note that $\check{\Gamma}$ is not necessarily contained in Γ , nor vice-versa, but are close in the following sense. For each $T^1 \in \mathcal{T}_{\partial,h}^1$ such that $\partial T^1 = E^1 \cup S^1$, where $E^1 \subset \partial \Gamma^1$ and S^1 are the interior edges, let $\check{T} := \Phi(T^1)$, $\check{E} := \Phi(E^1)$, $\check{S} := \Phi(S^1)$, and $E := \mathbf{F}_T(E^1) \subset \partial \Gamma$ (see Figure 3). Since E , \check{E} and E^1 interpolate Γ at the vertices of Γ^1 , then $\text{dist}(\mathbf{x}, E) = O(h^2)$ for all $\mathbf{x} \in \check{E}$.

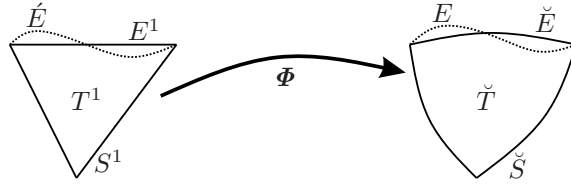


FIG. 3. Illustration of the closest point mapping of T^1 to Γ^* . The pre-image of the boundary edge $E \subset \partial \Gamma$ (dotted curve) is \check{E} .

Next, for $h > 0$ sufficiently small and by the properties of $\Phi(\cdot)$, there is a unique curve \check{E} that lies in the plane of T^1 such that $E \equiv \Phi(\check{E})$. Moreover, for h sufficiently small, $\check{E} = \Theta(E^1)$, where $\Theta(\bar{\mathbf{x}}) := \bar{\mathbf{x}} + \nu(\bar{\mathbf{x}})\bar{\mathbf{n}}(\bar{\mathbf{x}})$ for all $\bar{\mathbf{x}} \in E^1$, where $\bar{\mathbf{n}}$ is the outer co-normal of T^1 and $\nu \in C^2(E^1; \mathbb{R})$ such that $\nu|_{\partial E^1} = 0$. Therefore, there exists a unique flat triangle \check{T} in the plane of T^1 such that $\partial \check{T} = \check{E} \cup S^1$. This induces a triangle \check{T} in Γ such that $\check{T} := \Phi(\check{T})$ and $\partial \check{T} = E \cup \check{S}$. It is straightforward to prove the following result.

PROPOSITION 3.2 Consider the triangles \check{T}, \check{T} defined above from any given $T^1 \in \mathcal{T}_{\partial,h}^1$. Assume that $h > 0$ is small enough (depending on ρ) so that $\Gamma^1 \subset \mathcal{N}_\Gamma$ and the construction of \check{T} is well-defined. Then,

$$\check{T} \subset \Gamma, \quad \partial \check{T} \cap \partial \Gamma \in \mathcal{E}_{\partial,h}, \quad |\check{T} \Delta \check{T}| = O(h^3). \quad (3.5)$$

Furthermore, let $\check{\mathcal{T}}_{\partial,h} := \{\check{T}\}$ be generated from all $T^1 \in \mathcal{T}_{\partial,h}^1$, and define $\check{\mathcal{T}}_h := \{\check{T} \in \check{\mathcal{T}}_h \mid \check{T} \notin \check{\mathcal{T}}_{\partial,h}\} \cup \check{\mathcal{T}}_{\partial,h}$. Then, $\check{\mathcal{T}}_h$ gives an exact, conforming, shape regular triangulation of Γ .

Next, we have a procedure to “lift” a function from $T^1 \in \mathcal{T}_{\partial,h}^1$ to the corresponding $\check{T} \in \check{\mathcal{T}}_h$. Let $v : T^1 \rightarrow \mathbb{R}$ be given and define the lifted version $\check{v} : \check{T} \rightarrow \mathbb{R}$ (uniquely) such that $\check{v} \circ \Phi(\mathbf{x}) = v(\mathbf{x})$, for all $\mathbf{x} \in T^1$. And $v : \Gamma^1 \rightarrow \mathbb{R}$ is lifted to $\check{v} : \check{\Gamma} \rightarrow \mathbb{R}$, element-wise. Furthermore, recalling (3.5), for any $v \in C^2(\check{T} \cup \check{T})$ we have the estimates

$$\begin{aligned} \|v\|_{L^2(E)} &= [1 + O(h^2)] \|v\|_{L^2(\check{E})} + O(h^{5/2}) \|\nabla_{\Gamma^*} v\|_{L^\infty(\check{T} \Delta \check{T})}, \\ \|\nabla_{\Gamma} v\|_{L^2(E)} &= [1 + O(h^2)] \|\nabla_{\check{\Gamma}} v\|_{L^2(\check{E})} + O(h^{5/2}) \|\nabla_{\Gamma^*} \nabla_{\Gamma^*} v\|_{L^\infty(\check{T} \Delta \check{T})}, \end{aligned} \quad (3.6)$$

where we map \check{E} to $E \subset \partial \Gamma$ using the closest point map to E .

3.3.2 Element-wise Parametrization by the Closest Point Map. The Jacobian has a nice structure when using Φ . For simplicity, we drop “*” from \mathbf{v}^* , and note $\nabla \Phi(\mathbf{x}) = \mathbf{I}_3 - \mathbf{v}(\mathbf{x}) \otimes \mathbf{v}(\mathbf{x}) - \phi(\mathbf{x}) \mathbf{H}(\mathbf{x}) =$

$\mathbf{P}(\mathbf{x}) - \phi(\mathbf{x})\mathbf{H}(\mathbf{x})$, where $\mathbf{H} = \nabla \mathbf{v}$ is a symmetric matrix, $\mathbf{P}\mathbf{H} = \mathbf{H}\mathbf{P} = \mathbf{H}$, and further note that $\nabla_{T^1}\Phi = (\nabla\Phi)\bar{\mathbf{P}}$, and $\mathbf{J} = (\nabla_{T^1}\Phi)\bar{\mathbf{P}}_*$. Moreover, we have the identity

$$\mathbf{J} - \bar{\mathbf{P}}_* = [\mathbf{P}(\mathbf{x})\bar{\mathbf{P}} - \phi(\mathbf{x})\mathbf{H}(\mathbf{x})\bar{\mathbf{P}} - \mathbf{I}_3] \bar{\mathbf{P}}_* = -[\phi(\mathbf{x})\mathbf{H}(\mathbf{x}) + \mathbf{v}(\mathbf{x}) \otimes (\mathbf{v}(\mathbf{x}) - \bar{\mathbf{v}})] \bar{\mathbf{P}}_*. \quad (3.7)$$

In addition, the metric also has a nice structure:

$$\begin{aligned} \mathbf{g} &= \mathbf{J}^T \mathbf{J} = \bar{\mathbf{P}}_*^T \bar{\mathbf{P}} [\mathbf{P} - 2\phi\mathbf{H} + \phi^2(\mathbf{H})^2] \bar{\mathbf{P}} \bar{\mathbf{P}}_* = \mathbf{I}_2 + \bar{\mathbf{P}}_*^T \bar{\mathbf{P}} [\mathbf{P} - \bar{\mathbf{P}}] \bar{\mathbf{P}} \bar{\mathbf{P}}_* + O(h^2) \\ &= \mathbf{I}_2 + \bar{\mathbf{P}}_*^T \bar{\mathbf{P}} [(\mathbf{v} - \bar{\mathbf{v}}) \otimes (\mathbf{v} - \bar{\mathbf{v}})] \bar{\mathbf{P}} \bar{\mathbf{P}}_* + O(h^2) = \mathbf{I}_2 + O(h^2). \end{aligned} \quad (3.8)$$

Hence, for any $\bar{v} : T^1 \rightarrow \mathbb{R}$, the above results give the “lifted” surface gradient:

$$\begin{aligned} \nabla_{\check{\Gamma}} \check{v} \circ \Phi(\mathbf{x}) &= (\nabla_{T^1} \bar{v}) \bar{\mathbf{P}}_* \mathbf{g}^{-1} \mathbf{J}^T = (\nabla_{T^1} \bar{v}) \bar{\mathbf{P}}_* \mathbf{g}^{-1} \bar{\mathbf{P}}_*^T + (\nabla_{T^1} \bar{v}) \bar{\mathbf{P}}_* \mathbf{g}^{-1} (\mathbf{J} - \bar{\mathbf{P}}_*)^T \\ &= \nabla_{T^1} \bar{v} [\mathbf{I}_3 - (\mathbf{v}(\mathbf{x}) - \bar{\mathbf{v}}) \otimes \mathbf{v}(\mathbf{x}) + O(h^2)], \end{aligned} \quad (3.9)$$

and note that $\mathbf{n} \cdot \nabla_{\check{\Gamma}} \check{v} \circ \Phi(\mathbf{x}) = \bar{\mathbf{n}} \cdot \nabla_{T^1} \bar{v} + O(h^2)$.

Next, we lift the surface Hessian (recall (3.3)); for this, we need the surface Γ to be $C^{2,1}$. We start with

$$\begin{aligned} \nabla(\Phi \cdot \mathbf{a}_i) &= \mathbf{a}_i^T - (\mathbf{a}_i \cdot \mathbf{v}) \mathbf{v}^T - \phi(\mathbf{x}) \mathbf{a}_i^T \mathbf{H}(\mathbf{x}), \\ \nabla \nabla(\Phi \cdot \mathbf{a}_i) &= -\mathbf{v} \otimes \mathbf{H} \mathbf{a}_i - \mathbf{H} \mathbf{a}_i \otimes \mathbf{v} - (\mathbf{a}_i \cdot \mathbf{v}) \mathbf{H} - \phi(\mathbf{x}) \nabla(\mathbf{H} \mathbf{a}_i), \end{aligned} \quad (3.10)$$

and note that $\nabla_{T^1} \nabla_{T^1}(\Phi \cdot \mathbf{a}_i) = \bar{\mathbf{P}}(\nabla \nabla(\Phi \cdot \mathbf{a}_i)) \bar{\mathbf{P}}$. We now apply basic estimates to (3.3):

$$\begin{aligned} (\nabla_{\check{\Gamma}} \nabla_{\check{\Gamma}} \check{v}) \circ \Phi &= \nabla_{T^1} \nabla_{T^1} \bar{v} (1 + O(h)) + O(h) ((\nabla_{\check{\Gamma}} \check{v} \circ \Phi(\mathbf{x})) \cdot \mathbf{a}_i) \nabla \nabla(\Phi \cdot \mathbf{a}_i) \\ &\quad - ((\nabla_{\check{\Gamma}} \check{v} \circ \Phi(\mathbf{x})) \cdot \mathbf{P} \mathbf{a}_i) \mathbf{P}(\nabla \nabla(\Phi \cdot \mathbf{a}_i)) \mathbf{P}, \end{aligned} \quad (3.11)$$

and the second term equals $\phi((\nabla_{\check{\Gamma}} \check{v} \circ \Phi(\mathbf{x})) \cdot \mathbf{P} \mathbf{a}_i) \mathbf{P}(\nabla(\mathbf{H} \mathbf{a}_i)) \mathbf{P}$, where we note that $\sum_{i=1}^3 ((\nabla_{\check{\Gamma}} \check{v} \circ \Phi(\mathbf{x})) \cdot \mathbf{P} \mathbf{a}_i) (\mathbf{a}_i \cdot \mathbf{v}) = 0$. Thus, we obtain

$$(\nabla_{\check{\Gamma}} \nabla_{\check{\Gamma}} \check{v}) \circ \Phi = \nabla_{T^1} \nabla_{T^1} \bar{v} (1 + O(h)) + O(h) |\nabla_{T^1} \bar{v}| \mathbf{I}, \quad (3.12)$$

where the constants depend on $|\mathbf{H}|$ and $|h\nabla\mathbf{H}|$. If we had used the standard chart map, we would have obtained a similar estimate, except the lower order $|\nabla_{T^1} \bar{v}|$ term would have an $O(1)$ factor instead.

4. Mesh-dependent Estimates on Piecewise Linear Surfaces

The results in this section are an extension of the results in Section 2.4 to piecewise linear approximations of Γ . Let $\|\cdot\|_{2,h,1}$ denote the norm in (2.7) but defined on Γ^1 . Theorem 4.1 gives an elementary estimate for how $\|\cdot\|_{2,h}$ transforms between Γ^1 and Γ .

THEOREM 4.1 Set $m, l \in \{1, \infty\}$ with $m \neq l$. Let $v \in H_h^2(\Gamma^m)$, and define $\tilde{v} = v \circ \mathbf{F} \in H_h^2(\Gamma^l)$ if $l = 1$ or $\tilde{v} = v \circ \mathbf{F}^{-1} \in H_h^2(\Gamma^l)$ if $l = \infty$. Then,

$$\begin{aligned} \|\nabla_{\Gamma^m} \nabla_{\Gamma^m} v\|_{L^2(\mathcal{J}_h^m)} &\leq C \left(\|\nabla_{\Gamma^l} \nabla_{\Gamma^l} \tilde{v}\|_{L^2(\mathcal{J}_h^l)} + \|\nabla_{\Gamma^l} \tilde{v}\|_{L^2(\Gamma^l)} \right), \\ \|v\|_{2,h,m} &\leq C \left(\|\tilde{v}\|_{2,h,l} + \|\nabla_{\Gamma^l} \tilde{v}\|_{L^2(\Gamma^l)} \right), \end{aligned} \quad (4.1)$$

for some constant $C > 0$ depending only on the domain.

Proof. W.L.O.G., assume $m = \infty, l = 1$. A surface version of (Lenoir, 1986, Prop. 4) gives $\|v\|_{H^s(\Gamma^m)} \approx \|\tilde{v}\|_{H^s(\Gamma^l)}$ for $s \geq 0$. More specifically, $\|\nabla_\Gamma v\|_{L^2(\mathcal{T}_h)} \approx \|\nabla_{\Gamma^1} \tilde{v}\|_{L^2(\mathcal{T}_h^1)}$ and

$$\|\nabla_\Gamma \nabla_\Gamma v\|_{L^2(\mathcal{T}_h)} \leq C \left(\|\nabla_{\Gamma^1} \nabla_{\Gamma^1} \tilde{v}\|_{L^2(\mathcal{T}_h^1)} + \|\nabla_{\Gamma^1} \tilde{v}\|_{L^2(\mathcal{T}_h^1)} \right).$$

Applying a change of variables to the jump term in (2.7) gives

$$\|[\mathbf{n} \cdot \nabla_\Gamma v]\|_{L^2(\mathcal{E}_h)} \leq Ch \|\nabla_{\Gamma^1} \tilde{v}\|_{L^2(\mathcal{E}_h^1)} + \|[\hat{\mathbf{n}} \cdot \nabla_{\Gamma^1} \tilde{v}]\|_{L^2(\mathcal{E}_h^1)}, \quad (4.2)$$

where we emphasize that we cannot put a jump in the first term on the right-hand-side because different Jacobians appear on either side of the edge. Next, we have the following scaling estimate (see (2.5))

$\|\nabla_{\Gamma^1} \tilde{v}\|_{L^2(\partial\Gamma^1)}^2 \leq C_0 \left(h^{-1} \|\nabla_{\Gamma^1} \tilde{v}\|_{L^2(\Gamma^1)}^2 + h \|\nabla_{\Gamma^1} \nabla_{\Gamma^1} \tilde{v}\|_{L^2(\Gamma^1)}^2 \right)$, which leads to

$$\begin{aligned} h^{-1/2} \|[\mathbf{n} \cdot \nabla_\Gamma v]\|_{L^2(\mathcal{E}_h)} &\leq \\ C_1 \|\nabla_{\Gamma^1} \tilde{v}\|_{L^2(\mathcal{T}_h^1)} + C_1 h \|\nabla_{\Gamma^1} \nabla_{\Gamma^1} \tilde{v}\|_{L^2(\mathcal{T}_h^1)} + h^{-1/2} \|[\hat{\mathbf{n}} \cdot \nabla_{\Gamma^1} \tilde{v}]\|_{L^2(\mathcal{E}_h^1)}, \end{aligned} \quad (4.3)$$

and implies $\|v\|_{2,h} \leq C_2 \left(\|\tilde{v}\|_{2,h,1} + \|\nabla_{\Gamma^1} \tilde{v}\|_{L^2(\Gamma^1)} \right)$, giving the second inequality in (4.1). \square

Theorem 4.2 yields useful trace and Poincaré inequalities for the $\|\cdot\|_{2,h,1}$ norm on piecewise linear surfaces; in particular, (4.5) is the main result of this paper when free boundary conditions are present (i.e. $|\Sigma_f| > 0$).

THEOREM 4.2 Let $m = 1$ or ∞ . For all $v \in H_h^2(\Gamma^m)$, there holds

$$\begin{aligned} \|v\|_{L^\infty(\Gamma^m)} &\leq C_{\text{inf}} \left(\|v\|_{H^1(\Gamma^m)}^2 + \|\nabla_{\Gamma^m} \nabla_{\Gamma^m} v\|_{L^2(\mathcal{T}_h^m)}^2 \right)^{1/2}, \\ \|\nabla_{\Gamma^m} v\|_{L^2(\partial\Gamma^m)} &\leq C_{\text{tr}} \left(\|\nabla_{\Gamma^m} v\|_{L^2(\Gamma^m)}^2 + \|\nabla_{\Gamma^m} \nabla_{\Gamma^m} v\|_{L^2(\mathcal{T}_h^m)}^2 \right)^{1/2}, \end{aligned} \quad (4.4)$$

for constants $C_{\text{inf}}, C_{\text{tr}} > 0$ independent of h . Moreover, $\|\cdot\|_{2,h,m}$ is a norm on \mathcal{W}_h^m , and for $h > 0$ sufficiently small (depending only on Γ), there is a constant $C_P > 0$, depending only on Γ and independent of h , such that

$$\|v\|_{L^2(\Gamma^m)} + \|\nabla_{\Gamma^m} v\|_{L^2(\Gamma^m)} \leq C_P \|v\|_{2,h,m}, \text{ for all } v \in \mathcal{W}_h^m. \quad (4.5)$$

Proof. The $m = \infty$ case is done in Propositions 2.1, 2.2, and 2.3, so we only consider $m = 1$. Let $\tilde{v} \in H_h^2(\Gamma)$ and v be the corresponding mapped function in $H_h^2(\Gamma^1)$. Then, using (2.9), we have

$$\begin{aligned} \|v\|_{L^\infty(\Gamma^1)} &= \|\tilde{v}\|_{L^\infty(\Gamma)} \leq C \left(\|\tilde{v}\|_{H^1(\Gamma)}^2 + \|\nabla_\Gamma \nabla_\Gamma \tilde{v}\|_{L^2(\mathcal{T}_h)}^2 \right)^{1/2} \\ &\leq C \left(\|v\|_{H^1(\Gamma^1)}^2 + \|\nabla_{\Gamma^1} \nabla_{\Gamma^1} v\|_{L^2(\mathcal{T}_h^1)}^2 \right)^{1/2}, \end{aligned} \quad (4.6)$$

where we used (4.1) and that $\|v\|_{H^1(\Gamma^1)} \approx \|\tilde{v}\|_{H^1(\Gamma)}$; this proves the first inequality in (4.4). The trace inequality follows by noting $\|\nabla_{\Gamma^1} v\|_{L^2(\partial\Gamma^1)} \approx \|\nabla_\Gamma \tilde{v}\|_{L^2(\partial\Gamma)}$, $\|\nabla_{\Gamma^1} v\|_{L^2(\Gamma^1)} \approx \|\nabla_\Gamma \tilde{v}\|_{L^2(\Gamma)}$ and using (2.10) together with (4.1).

Next, specialize $v \in H_h^2(\Gamma^1)$ to be a continuous, piecewise linear function on Γ^1 and lift it to $\check{\Gamma}$, i.e. $\check{v} \in H_h^2(\check{\Gamma}, \check{\mathcal{T}}_h)$, where $\check{v} \circ \Phi = v$, with Φ the closest point map from Section 3.3.1. Since v is linear

on each $T^1 \in \mathcal{T}_h^1$, there is a natural way to continuously extend \check{v} to Γ , wherever necessary. Ergo, $\check{v} \in H_h^2(\Gamma, \check{\mathcal{T}}_h)$. Thus, we can apply (2.12)

$$\begin{aligned} \|\nabla_\Gamma \check{v}\|_{L^2(\Gamma)} &\leq \dot{C}_P \left(\|\nabla_\Gamma \nabla_\Gamma \check{v}\|_{L^2(\check{\mathcal{T}}_h)}^2 + \|\check{v}\|_{L^2(\Sigma_c \cup \Sigma_s)}^2 + \Xi^2(\check{v}) \right. \\ &\quad \left. + h^{-1} \|\llbracket \check{\mathbf{n}} \cdot \nabla_\Gamma \check{v} \rrbracket\|_{L^2(\check{\mathcal{E}}_{0,h})}^2 + h^{-1} \|\check{\mathbf{n}} \cdot \nabla_\Gamma \check{v}\|_{L^2(\Sigma_c)}^2 \right)^{1/2}, \end{aligned} \quad (4.7)$$

where \dot{C}_P depends on the shape regularity of $\check{\mathcal{T}}_h$; note that the boundary terms are on $\partial\Gamma$. Accounting for the ‘‘skin’’ $\check{T} \setminus \check{T}$, where necessary, and using (3.6), we get

$$\begin{aligned} \|\nabla_\Gamma \check{v}\|_{L^2(\Gamma)} &\leq C \left(\|\nabla_{\check{T}} \nabla_{\check{T}} \check{v}\|_{L^2(\check{\mathcal{T}}_h)}^2 + \|\check{v}\|_{L^2(\check{\Sigma}_c \cup \check{\Sigma}_s)}^2 + \Xi^2(\check{v}) \right. \\ &\quad \left. + h^{-1} \|\llbracket \check{\mathbf{n}} \cdot \nabla_{\check{T}} \check{v} \rrbracket\|_{L^2(\check{\mathcal{E}}_{0,h})}^2 + h^{-1} \|\check{\mathbf{n}} \cdot \nabla_{\check{T}} \check{v}\|_{L^2(\check{\Sigma}_c)}^2 \right)^{1/2} + A_1, \end{aligned} \quad (4.8)$$

where

$$A_1^2 \leq C \sum_{\check{T} \in \check{\mathcal{T}}_{\partial,h}} \left(\|\nabla_\Gamma \nabla_\Gamma \check{v}\|_{L^2(\check{T} \setminus \check{T})}^2 + h^5 \|\nabla_{\check{T}} \check{v}\|_{L^\infty(\check{T} \setminus \check{T})}^2 + h^4 \|\nabla_{\check{T}} \nabla_{\check{T}} \check{v}\|_{L^\infty(\check{T} \setminus \check{T})}^2 \right). \quad (4.9)$$

Since \check{v} is a (mapped) piecewise linear function, using an inverse estimate and (3.5) shows that $\|\nabla_\Gamma \nabla_\Gamma \check{v}\|_{L^2(\check{T} \setminus \check{T})}^2 = O(h) \|\nabla_{\check{T}} \nabla_{\check{T}} \check{v}\|_{L^2(\check{T})}^2$ and

$$Ch^2 \|\nabla_{\check{T}} \check{v}\|_{L^\infty(\check{T} \setminus \check{T})}^2 = \|\nabla_{\check{T}} \check{v}\|_{L^2(\check{T})}^2, \quad Ch^2 \|\nabla_{\check{T}} \nabla_{\check{T}} \check{v}\|_{L^\infty(\check{T} \setminus \check{T})}^2 = \|\nabla_{\check{T}} \nabla_{\check{T}} \check{v}\|_{L^2(\check{T})}^2. \quad (4.10)$$

Thus, $A_1^2 \leq Ch \left(\|\nabla_{\check{T}} \nabla_{\check{T}} \check{v}\|_{L^2(\check{\mathcal{T}}_{\partial,h})}^2 + h^2 \|\nabla_{\check{T}} \check{v}\|_{L^2(\check{\mathcal{T}}_{\partial,h})}^2 \right)$. Now, by mapping from \check{T} to Γ^1 and utilizing (3.9) and (3.12), the estimate (4.8) reduces to

$$\begin{aligned} \|\nabla_\Gamma \check{v}\|_{L^2(\Gamma)} &\leq C \left(\|\nabla_{\Gamma^1} \nabla_{\Gamma^1} v\|_{L^2(\mathcal{T}_h^1)}^2 + \|v\|_{L^2(\Sigma_c^1 \cup \Sigma_s^1)}^2 + \Xi^2(v) + h^{-1} \|\llbracket \check{\mathbf{n}} \cdot \nabla_{\Gamma^1} v \rrbracket\|_{L^2(\mathcal{E}_{0,h}^1)}^2 \right. \\ &\quad \left. + h^{-1} \|\check{\mathbf{n}} \cdot \nabla_{\Gamma^1} v\|_{L^2(\Sigma_c^1)}^2 \right)^{1/2} + Ch \|\nabla_{\Gamma^1} v\|_{L^2(\Gamma^1)}, \end{aligned} \quad (4.11)$$

where we note that $\Xi(\check{v}) \equiv \Xi(v)$. Since $\|\nabla_{\Gamma^1} v\|_{L^2(\Gamma^1)} \leq C \|\nabla_\Gamma \check{v}\|_{L^2(\Gamma)}$, for h sufficiently small depending on the $C^{2,1}$ norm of Γ , we obtain

$$\|\nabla_{\Gamma^1} v\|_{L^2(\Gamma^1)} \leq C'_P \|v\|_{h,1}, \quad (4.12)$$

for all continuous, piecewise linear functions on Γ^1 , where $\|\cdot\|_{h,1}$ is the same as $\|\cdot\|_h$ in Proposition 2.2 except defined on Γ^1 .

Next, let w be any function in $H_h^2(\Gamma^1)$. Then, by (4.12) and approximation theory,

$$\begin{aligned} \|\nabla_{\Gamma^1} w\|_{L^2(\Gamma^1)} &\leq \|\nabla_{\Gamma^1} \mathcal{I}_h w\|_{L^2(\Gamma^1)} + \|\nabla_{\Gamma^1} (w - \mathcal{I}_h w)\|_{L^2(\Gamma^1)} \\ &\leq C'_P \|\mathcal{I}_h w\|_{h,1} + Ch \|w\|_{2,h,1} \leq C \|w\|_{h,1}, \end{aligned} \quad (4.13)$$

where \mathcal{I}_h is the standard continuous linear, nodal Lagrange interpolation operator. Note that the pointwise terms in $\|\cdot\|_{h,1}$ vanish when restricting to the space \mathcal{W}_h^m . This proves the H^1 inequality in (4.5).

Note: in the case that $\partial\Gamma = \emptyset$, or $\Sigma_f = \emptyset$, the result can be derived by a simple integration by parts argument, and Γ only need be C^2 . Lastly, applying similar mapping arguments to (2.11) yields

$$\|v\|_{L^2(\Gamma^1)} \leq C \left(\|\nabla_{\Gamma^1} v\|_{L^2(\Gamma^1)}^2 + \|v\|_{h,1}^2 \right)^{1/2}. \quad (4.14)$$

Ergo, the L^2 inequality in (4.5) follows by combining (4.14) with the H^1 inequality (4.13). \square

REMARK 4.1 (kernel of the Hessian) The purpose of the point condition $\Xi(w) = 0$ is to control the kernel of the broken Hessian $\nabla_{\Gamma^m} \nabla_{\Gamma^m}$. Alternative conditions could also be used. For example, if $m = \infty$ and uniformly free conditions, $\Sigma \equiv \Sigma_f$, are imposed, then one can set $\mathcal{W}_h := H_h^2(\Gamma) / \ker(\nabla_{\Gamma} \nabla_{\Gamma})$ (quotient space). This gives the space of $H_h^2(\Gamma)$ functions that are orthogonal to constants and any Killing fields that Γ may have. However, setting point conditions are usually more convenient with conforming finite element spaces (see (4.16)).

Furthermore, in general, $\ker(\nabla_{\Gamma} \nabla_{\Gamma}) \neq \ker(\nabla_{\Gamma^1} \nabla_{\Gamma^1})$, i.e. the kernel of the broken Hessian on the true domain Γ is usually not the same as on the piecewise linear approximation Γ^1 . In fact, it is possible that $\dim(\ker(\nabla_{\Gamma} \nabla_{\Gamma})) \neq \dim(\ker(\nabla_{\Gamma^1} \nabla_{\Gamma^1}))$. The kernel of the broken Hessian on a triangulated surface involves jump conditions of the co-normal derivative across the edges. Indeed, the topology of the mesh could affect the kernel. Therefore, it is better to simply set point conditions, that do not depend on h , that are known to control $\ker(\nabla_{\Gamma} \nabla_{\Gamma})$ on the true domain. This ensures convergence, e.g. for a finite element discretization of a 4th order elliptic problem on surfaces, see Walker (2020).

THEOREM 4.3 Assume the hypothesis of Theorem 4.1. Then, for $h > 0$ sufficiently small,

$$C^{-1} \|\hat{v}\|_{2,h,l} \leq \|v\|_{2,h,m} \leq C \|\hat{v}\|_{2,h,l}, \quad \text{for all } v \in \mathcal{W}_h^m, \quad (4.15)$$

where $C > 0$ depends only on Γ .

Proof. Inequality (4.15) follows by combining (4.1) and (4.5). \square

REMARK 4.2 Let $r \geq 0$ be an integer and $m = 1$ or ∞ . The (continuous) Lagrange finite element space of degree $r + 1$ on Γ^m is defined via the mapping $\mathcal{Q}_T := \mathbf{F}_T$, if $m = \infty$, or $\mathcal{Q}_T := \text{id}_{T^1}$, if $m = 1$:

$$S_h^m \equiv S_h^m(\Gamma^m) := \{v \in H_h^2(\Gamma^m) \mid v|_T \circ \mathcal{Q}_T \in \mathcal{P}_{r+1}(T^1), \forall T \in \mathcal{T}_h^m\}. \quad (4.16)$$

For the case $m = \infty$ (i.e. the true domain) we simply write S_h . Clearly, $S_h^m \subset H_h^2(\Gamma^m)$. Thus, $W_h^m := S_h^m \cap \{v \in H^1(\Gamma) \mid v = 0 \text{ on } \Sigma_c \cup \Sigma_s, \Xi(v) = 0\}$ is a subspace of \mathcal{W}_h^m and so the above results apply to the finite element space W_h^m as well.

5. Conclusion

We presented several useful estimates for mesh dependent H^2 spaces on piecewise linear surface triangulations with boundary. Our analysis used the closest point map, which enjoys nice properties, to establish a crucial Poincaré inequality in (4.5) when free boundary conditions are present (see Section 3.3). In doing this, we adapted the (classic) closest point map technique to work on surfaces with boundary. The results presented here should be useful for analyzing non-conforming H^2 type FEMs, i.e. for approximating fourth order elliptic problems on surfaces with boundary by non-conforming FEMs posed on piecewise linear triangulations, or even piecewise polynomial surfaces. For example, see the surface finite element scheme in Walker (2020) for the Kirchhoff plate problem posed on a surface.

- ADAMS, R. A. & FOURNIER, J. J. F. (2003) *Sobolev Spaces*. Pure and Applied Mathematics Series, vol. 140, 2nd edn. Elsevier.
- AGMON, S. (1965) *Lectures on elliptic boundary value problems*. Van Nostrand mathematical studies: no. 2. Van Nostrand.
- ARNOLD, D. N. & WALKER, S. W. (2020) The hellan–herrmann–johnson method with curved elements. *SIAM Journal on Numerical Analysis*, **58**, 2829–2855.
- ARNOLD, D. N. & BREZZI, F. (1985) Mixed and nonconforming finite element methods : implementation, postprocessing and error estimates. *ESAIM: M2AN*, **19**, 7–32.
- BABUŠKA, I., OSBORN, J. & PITKÄRANTA, J. (1980) Analysis of mixed methods using mesh dependent norms. *Mathematics of Computation*, **35**, 1039–1062.
- BÄNSCH, E., MORIN, P. & NOCHETTO, R. H. (2005) A finite element method for surface diffusion: the parametric case. *Journal of Computational Physics*, **203**, 321–343.
- BARRETT, J. W., GARCKE, H. & NÜRNBERG, R. (2010) On stable parametric finite element methods for the stefan problem and the mullins-sekerka problem with applications to dendritic growth. *Journal of Computational Physics*, **229**, 6270–6299.
- BARRETT, J. W., GARCKE, H. & NÜRNBERG, R. (2015) A stable parametric finite element discretization of two-phase navier-stokes flow. *Journal of Scientific Computing*, **63**, 78–117.
- BARRETT, J. W., GARCKE, H. & NÜRNBERG, R. (2016) A stable numerical method for the dynamics of fluidic membranes. *Numerische Mathematik*, **134**, 783–822.
- BLUM, H. & RANNACHER, R. (1990) On mixed finite element methods in plate bending analysis. part 1: The first herrmann scheme. *Computational Mechanics*, **6**, 221–236.
- BONITO, A., NOCHETTO, R. H. & SEBASTIAN PAULETTI, M. (2010) Parametric fem for geometric biomembranes. *J. Comput. Phys.*, **229**, 3171–3188.
- BONITO, A., NOCHETTO, R. & PAULETTI, M. (2011) Dynamics of biomembranes: Effect of the bulk fluid. *Mathematical Modelling of Natural Phenomena*, **6**, 25–43.
- BRENNER, S. C. & SCOTT, L. R. (2008) *The Mathematical Theory of Finite Element Methods*. Texts in Applied Mathematics, vol. 15, 3rd edn. New York, NY: Springer.
- BREZZI, F. & RAVIART, P. A. (1976) Mixed finite element methods for 4th order elliptic equations. *Topics In Numerical Analysis III: Proceedings of the Royal Irish Academy Conference on Numerical Analysis* (J. J. H. Miller ed.). Academic Press, pp. 33–56.
- BURMAN, E., HANSBO, P., LARSON, M. G., LARSSON, K. & MASSING, A. (2019) Finite element approximation of the laplace–beltrami operator on a surface with boundary. *Numerische Mathematik*, **141**, 141–172.
- CIARLET, P. G. (2013) *Linear and Nonlinear Functional Analysis with Applications*, 1st edn. SIAM.
- COMODI, M. I. (1989) The Hellan–Herrmann–Johnson method: Some new error estimates and postprocessing. *Mathematics of Computation*, **52**, 17–29.
- DAVIS, C. B. & WALKER, S. W. (2015) A mixed formulation of the Stefan problem with surface tension. *Interfaces and Free Boundaries*, **17**, 427–464.
- DAVIS, C. B. & WALKER, S. W. (2017) Semi-discrete error estimates and implementation of a mixed method for the Stefan problem. *ESAIM: Mathematical Modelling and Numerical Analysis*, **51**, 2093 – 2126.
- DECKELNICK, K., DZIUK, G. & ELLIOTT, C. M. (2005) Computation of geometric partial differential equations and mean curvature flow. *Acta Numerica*, **14**, 139–232.
- DELFOUR, M. C. & ZOLÉSIO, J.-P. (2011) *Shapes and Geometries: Analysis, Differential Calculus, and Optimization*. Advances in Design and Control, vol. 4, 2nd edn. SIAM.
- DEMLow, A. (2009) Higher-order finite element methods and pointwise error estimates for elliptic problems on surfaces. *SIAM Journal on Numerical Analysis*, **47**, 805–827.
- DEMLow, A. & DZIUK, G. (2007) An adaptive finite element method for the laplace–beltrami operator on implicitly defined surfaces. *SIAM Journal on Numerical Analysis*, **45**, 421–442.

- DO CARMO, M. P. (1976) *Differential Geometry of Curves and Surfaces*. Upper Saddle River, New Jersey: Prentice Hall.
- DO CARMO, M. P. (1992) *Riemannian Geometry*. Mathematics: Theory and Applications, 2nd (english) edn. Boston: Birkhäuser.
- DU, Q., LIU, C. & WANG, X. (2004) A phase field approach in the numerical study of the elastic bending energy for vesicle membranes. *Journal of Computational Physics*, **198**, 450.
- DU, Q., LIU, C., RYHAM, R. & WANG, X. (2005) A phase field formulation of the willmore problem. *Nonlinearity*, **18**, 1249.
- DZIUK, G. (1988) In S. Hildebrandt, R. Leis (eds): *Partial Differential Equations and Calculus of Variations*, vol. 1357. Springer, Berlin, Heidelberg, chapter Finite Elements For the Beltrami Operator On Arbitrary Surfaces, pp. 142–155.
- DZIUK, G. (2008) Computational parametric willmore flow. *Numerische Mathematik*, **111**, 55–80.
- DZIUK, G. & ELLIOTT, C. M. (2013) Finite element methods for surface pdes. *Acta Numerica*, **22**, 289–396.
- EISENHART, L. P. (1926) *Riemannian Geometry*. Princeton University Press.
- ELLIOTT, C. M., STINNER, B. & VENKATARAMAN, C. (2012) Modelling cell motility and chemotaxis with evolving surface finite elements. *Journal of The Royal Society Interface*, **9**, 3027–3044.
- ELLIOTT, C. M. & RANNER, T. (2015) Evolving surface finite element method for the cahn–hilliard equation. *Numerische Mathematik*, **129**, 483–534.
- ELLIOTT, C. M. & STINNER, B. (2010) Modeling and computation of two phase geometric biomembranes using surface finite elements. *Journal of Computational Physics*, **229**, 6585 – 6612.
- GERBEAU, J.-F. & LELIÈVRE, T. (2009) Generalized navier boundary condition and geometric conservation law for surface tension. *Computer Methods in Applied Mechanics and Engineering*, **198**, 644 – 656.
- GROMOV, M. (1991) Sign and geometric meaning of curvature. *Rendiconti del Seminario Matematico e Fisico di Milano*, **61**, 9–123.
- HEBEY, E. (1996) *Sobolev Spaces on Riemannian Manifolds*. Lecture Notes in Mathematics. Springer-Verlag Berlin Heidelberg.
- KREYSZIG, E. (1991) *Differential Geometry*. Dover.
- LARSSON, K. & LARSON, M. G. (2017) A continuous/discontinuous galerkin method and a priori error estimates for the biharmonic problem on surfaces. *Mathematics of Computation*, **86**, 2613–2649.
- LENOIR, M. (1986) Optimal isoparametric finite elements and error estimates for domains involving curved boundaries. *SIAM Journal of Numerical Analysis*, **23**, 562–580.
- PETERSEN, P. (2006) *Riemannian Geometry*. Graduate Texts in Mathematics, 2nd edn. Springer-Verlag.
- SMEREKA, P. (2003) Semi-implicit level set methods for curvature and surface diffusion motion. *Journal of Scientific Computing*, **19**, 439–456.
- WALKER, S. W., SHAPIRO, B. & NOCHETTO, R. H. (2009) Electrowetting with contact line pinning: Computational modeling and comparisons with experiments. *Physics of Fluids*, **21**, 102103.
- WALKER, S. W. (2015) *The Shapes of Things: A Practical Guide to Differential Geometry and the Shape Derivative*. Advances in Design and Control, vol. 28, 1st edn. SIAM.
- WALKER, S. W. (2020) The kirchhoff plate equation on surfaces: The surface hellan–herrmann–johnson method. *in review*.
- ZHONG-CAN, O.-Y. & HELFRICH, W. (1989) Bending energy of vesicle membranes: General expressions for the first, second, and third variation of the shape energy and applications to spheres and cylinders. *Phys. Rev. A*, **39**, 5280–5288.

A. Differential Geometry

In this appendix, we review the differential geometry tools needed for working on manifolds Kreyszig (1991); do Carmo (1992, 1976); Ciarlet (2013); Hebey (1996). Specifically, we review the basic notation

of covariant, contravariant, and other differential geometry concepts.

A.1 Intrinsic

For the sake of generality, consider a d -dimensional Riemannian manifold $(\Gamma, g_{\alpha\beta})$, where $g_{\alpha\beta}$ is the given metric tensor (discussed in Section A.1.2) defined over a (reference) domain $U \subset \mathbb{R}^d$; for simplicity of exposition, assume only one reference domain is needed to define the manifold (of course, this is not necessary). A point in U is denoted by (u^1, u^2, \dots, u^d) ; in the special case of $d = 2$ that we are mainly concerned with, we may use $(u, v) \in U$. We refer to variables defined on U as *intrinsic* quantities.

A.1.1 Tensor Index Notation. We use lower-case *Greek* indices (α, β, γ , etc.), which take values in $\{1, 2, \dots, d\}$ when referring to intrinsic variables. For example, ∂_α is the partial derivative with respect to the coordinate u^α for $\alpha \in \{1, 2, \dots, d\}$. Covariant vectors are denoted with *lower* indices, e.g. (v_1, v_2, \dots, v_d) and contravariant vectors are denoted with *upper* indices, e.g. (v^1, v^2, \dots, v^d) . The β -th component of a covariant (contravariant) derivative is denoted by ∇_β (∇^β).

Moreover, covariant and contravariant components of general *tensor* quantities use lower and upper Greek indices, respectively, e.g. $w_{\alpha\beta}$ (covariant tensor), $w^{\alpha\beta}$ (contravariant tensor), w_α^β , w_β^α (mixed tensor). We adopt the Einstein summation convention, i.e. repeated indices are summed over, e.g. $w^\alpha r_\alpha \equiv \sum_{\alpha=1}^d w^\alpha r_\alpha$, where one index is lower and the other is upper. E.g. it is not allowed to sum over two repeated *lower* indices. We use the Kronecker delta $\delta_{\alpha\beta}$, $\delta^{\alpha\beta}$, δ_α^β , etc., with appropriate upper/lower indices depending on the context.

Furthermore, we use the letters a-h (with a different font for emphasis) as a *non-numerical* label to indicate a covariant, contravariant, or mixed tensor. For example, v_a refers to a covariant vector (not just a single component), i.e. $v_a \equiv (v_1, \dots, v_d)$. Similarly, $\nabla^c z = (\nabla^1 z, \dots, \nabla^d z)$ refers to a contravariant vector, where z is a scalar quantity. For non-numerical labels, the specific symbol does not matter; it is simply a placeholder. When convenient, we use bold-face for vector and tensor quantities instead of writing out indices.

A.1.2 Main Concepts. The given metric $g_{\alpha\beta}$ is a symmetric, covariant tensor with component functions $g_{\alpha\beta} : U \rightarrow \mathbb{R}$, for $1 \leq \alpha, \beta \leq d$, which we assume are at least C^1 , and is uniformly positive definite. We write $g := \det g_{\alpha\beta}$ and the inverse metric tensor g^{ab} is contravariant with components denoted $g^{\alpha\beta}$, where $g_{\alpha\gamma} g^{\gamma\beta} = \delta_\alpha^\beta$. Note that v^a may be converted to v_b via $v_b = g_{b\alpha} v^\alpha$; similarly, w_b may be converted to w^a by $w^a = g^{a\beta} w_\beta$. When convenient, we write $g_{\alpha\beta} \equiv \mathbf{g} = [g_{\alpha\beta}]_{\alpha, \beta=1}^d$ and $g^{ab} \equiv \mathbf{g}^{-1} = [g^{\alpha\beta}]_{\alpha, \beta=1}^d$ in standard matrix notation for the metric and inverse metric, respectively. Let $\mathbb{T}_2 = \mathbb{T}_2(\Gamma)$ ($\mathbb{T}^2 = \mathbb{T}^2(\Gamma)$) be the set of covariant (contravariant) 2-tensors on Γ . Moreover, $\mathbb{S}_2 \subset \mathbb{T}_2$ and $\mathbb{S}^2 \subset \mathbb{T}^2$ are subsets of symmetric tensors; so then $g_{\alpha\beta} \in \mathbb{S}_2$ and $g^{ab} \in \mathbb{S}^2$.

The Christoffel symbols Γ_{ij}^k (of the second kind) are defined by

$$\Gamma_{\alpha\beta}^\gamma := \frac{1}{2} g^{\mu\gamma} (\partial_\alpha g_{\beta\mu} + \partial_\beta g_{\mu\alpha} - \partial_\mu g_{\alpha\beta}), \quad 1 \leq \alpha, \beta, \gamma \leq d, \quad (\text{A.1})$$

where $\Gamma_{\alpha\beta}^\gamma = \Gamma_{\beta\alpha}^\gamma$ do Carmo (1992, 1976). With this, we recall the definition of covariant (contravariant) derivatives, denoted ∇_α (∇^α), where f is a scalar, v_b is a covariant vector, and v^c is a contravariant

vector:

$$\begin{aligned}\nabla_\alpha f &= \partial_\alpha f, & \nabla_\alpha \nabla_\beta f &= \partial_\alpha \partial_\beta f - (\partial_\gamma f) \Gamma_{\alpha\beta}^\gamma, \\ \nabla_\alpha v_\beta &= \partial_\alpha v_\beta - v_\gamma \Gamma_{\beta\alpha}^\gamma, & \nabla_\alpha v^\gamma &= \partial_\alpha v^\gamma + v^\beta \Gamma_{\beta\alpha}^\gamma, & \nabla_\alpha v^\alpha &= (\sqrt{g})^{-1} \partial_\alpha (v^\alpha \sqrt{g}).\end{aligned}\tag{A.2}$$

The metric satisfies do Carmo (1992) $\nabla_\gamma g_{\alpha\beta} = 0$, $\nabla_\gamma g^{\alpha\beta} = 0$, $\nabla_\gamma g = 0$, for $1 \leq \alpha, \beta, \gamma \leq 2$. The “area” element on the manifold Γ is denoted $dS(g) = \sqrt{g} du \equiv \sqrt{g} du^1 \cdots du^d$, where du is the Lebesgue measure on \mathbb{R}^d . Viewing n_α as a “vector” in \mathbb{R}^d , it has unit length under the \mathbb{R}^d Euclidean metric. If $d = 2$, let t^α be the oriented (contravariant) tangent vector of ∂U , which has unit length in the Euclidean metric and satisfies $n_\alpha t^\alpha = 0$. Moreover, $g = t^\mu t_\mu / (n^\mu n_\mu)$, which implies that $ds(g) := \sqrt{t^\mu t_\mu} dl$ for $d = 2$, and we have the following “orthogonal” decomposition

$$\delta_\beta^\alpha = \frac{n^\alpha n_\beta}{n^\mu n_\mu} + \frac{t^\alpha t_\beta}{t^\mu t_\mu}.\tag{A.3}$$

A.2 Extrinsic

Suppose that the manifold Γ is embedded in \mathbb{R}^n , with $n \geq d$, and that it is represented by a family of charts $\{(U_i, \boldsymbol{\chi}_i)\}$, where a single chart consists of a pair $(U, \boldsymbol{\chi})$, with $U \subset \mathbb{R}^d$ (reference domain) and $\boldsymbol{\chi} : U \rightarrow \mathbb{R}^n$ do Carmo (1992). For simplicity of exposition, assume there is only one chart $(U, \boldsymbol{\chi})$, where $\Gamma = \boldsymbol{\chi}(U)$. We refer to variables in \mathbb{R}^n as *extrinsic* quantities.

A.2.1 Tensor Index Notation. We use lower-case *Latin* letters starting with i (i.e. i, j, k, l , etc.), which take values in $\{1, 2, \dots, n\}$, when referring to components of extrinsic (ambient space) quantities. For example, $\boldsymbol{\chi} = (\chi^1, \dots, \chi^n)^T \in \mathbb{R}^n$, and $\chi^i : U \rightarrow \mathbb{R}$ for each $i \in \{1, 2, \dots, n\}$. A point $\mathbf{x} \in \mathbb{R}^n$ has its j -th coordinate denoted by x^j . Moreover, ∂_k is the partial derivative with respect to coordinate x^k . Repeated indices are summed over. We typically bold-face extrinsic vectors and tensors, e.g. let \mathbf{w} be a (covariant) 2-tensor in \mathbb{R}^n with components w_{ij} for $i, j \in \{1, 2, \dots, n\}$. The canonical (orthonormal) basis in \mathbb{R}^n , is denoted by $\{\mathbf{a}_k\}_{k=1}^n$, where $\mathbf{a}_1 = (1, 0, \dots, 0)^T$ (column vector), etc. With the Kronecker delta δ_i^j , we have the dual basis $\{\mathbf{a}^k\}$ of $\{\mathbf{a}_k\}$ by the formula $\mathbf{a}_i \cdot \mathbf{a}^j = \delta_i^j$.

A.2.2 Differential Geometry in the Ambient Space. The tangent space $T_{\mathbf{x}}(\Gamma)$, at a point $\mathbf{x} \in \Gamma$, is a subspace of \mathbb{R}^n spanned by $\{\mathbf{e}_1, \mathbf{e}_2, \dots, \mathbf{e}_d\}$ (the covariant basis) where

$$\mathbf{e}_\alpha = \partial_\alpha \boldsymbol{\chi}(u^\alpha), \quad 1 \leq \alpha \leq d, \quad \text{where } u^\alpha \equiv (u^1, \dots, u^d) = \boldsymbol{\chi}^{-1}(\mathbf{x}).\tag{A.4}$$

In this case, the metric tensor $g_{\alpha\beta}$ is given by $g_{\alpha\beta} = \mathbf{e}_\alpha \cdot \mathbf{e}_\beta$, for $1 \leq \alpha, \beta \leq d$. The contravariant tangent basis is given by $\{\mathbf{e}^1, \mathbf{e}^2, \dots, \mathbf{e}^d\}$, where $\mathbf{e}^\beta = \mathbf{e}_\alpha g^{\alpha\beta} = (\partial_\alpha \boldsymbol{\chi}) g^{\alpha\beta}$ Ciarlet (2013). Sometimes, we express $g_{\alpha\beta} \equiv \mathbf{g} = \mathbf{J}^T \mathbf{J}$, where $\mathbf{J} = [\mathbf{e}_1, \dots, \mathbf{e}_d]$ is an $n \times d$ matrix.

Given a vector $\mathbf{v} \in \mathbb{R}^n$, it is in the tangent space $T_{\mathbf{x}}(\Gamma)$ if there exists a (contravariant) vector v^α such that $\mathbf{v}(\mathbf{x}) = v^\alpha \mathbf{e}_\alpha \circ \boldsymbol{\chi}^{-1}(\mathbf{x})$. Alternatively, one can write it in terms of a co-vector v_α and the contravariant basis: $\mathbf{v}(\mathbf{x}) = v_\alpha \mathbf{e}^\alpha \circ \boldsymbol{\chi}^{-1}(\mathbf{x})$. Moreover, any covariant (contravariant) vector v_α (v^α) has a corresponding *extrinsic version* given by $\mathbf{v} = v_\alpha \mathbf{e}^\alpha$ ($\mathbf{v} = v^\alpha \mathbf{e}_\alpha$). We define the tangent bundle:

$$T(\Gamma) = \{(\mathbf{x}, \mathbf{v}) \mid \mathbf{x} \in \Gamma, \mathbf{v}(\mathbf{x}) \in T_{\mathbf{x}}(\Gamma)\},\tag{A.5}$$

thus, we say $\mathbf{v} \in T(\Gamma)$ if $\mathbf{v}(\mathbf{x}) \in T_{\mathbf{x}}(\Gamma)$ for every $\mathbf{x} \in \Gamma$; in this case, we write $\mathbf{v} : \Gamma \rightarrow T(\Gamma)$.

Next, we introduce extrinsic differential operators via their intrinsic counterpart, starting with the surface gradient $\nabla_{\Gamma} f : \Gamma \rightarrow T(\Gamma)$ defined in local coordinates by

$$(\nabla_{\Gamma} f) \circ \boldsymbol{\chi} = (\nabla_{\alpha} f) g^{\alpha\beta} \mathbf{e}_{\beta}^T = \partial_{\alpha}(f \circ \boldsymbol{\chi}) g^{\alpha\beta} (\partial_{\beta} \boldsymbol{\chi})^T \equiv \nabla(f \circ \boldsymbol{\chi}) \mathbf{g}^{-1} \mathbf{J}^T. \quad (\text{A.6})$$

The (covariant) surface Hessian (a symmetric tensor) is given by

$$(\nabla_{\Gamma} \nabla_{\Gamma} f) \circ \boldsymbol{\chi} := \mathbf{e}_{\mu} g^{\mu\alpha} [\nabla_{\alpha} \nabla_{\beta} f] g^{\beta\rho} \mathbf{e}_{\rho}^T = \mathbf{e}_{\mu} g^{\mu\alpha} [\partial_{\alpha} \partial_{\beta}(f \circ \boldsymbol{\chi}) - \partial_{\gamma}(f \circ \boldsymbol{\chi}) \Gamma_{\alpha\beta}^{\gamma}] g^{\beta\rho} \mathbf{e}_{\rho}^T. \quad (\text{A.7})$$

A.2.3 Special Case of a Surface. Suppose $d = 2$ and $n = 3$. We have the following integration by parts relation:

$$\begin{aligned} \int_{\Gamma} f \nabla_{\Gamma} \cdot \mathbf{v} dS &= \int_{\partial\Gamma} f \mathbf{v} \cdot \mathbf{n} ds - \int_{\Gamma} (\nabla_{\Gamma} f) \cdot \mathbf{v} dS, \\ \int_{\Gamma} (\operatorname{div}_{\Gamma} \mathbf{r}) \cdot \nabla_{\Gamma} f dS &= \int_{\partial\Gamma} (\mathbf{n}^T \mathbf{r}) \cdot \nabla_{\Gamma} f ds - \int_{\Gamma} \mathbf{r} : \nabla_{\Gamma} \nabla_{\Gamma} f dS, \end{aligned} \quad (\text{A.8})$$

where we suppress the g dependence in the differential measure and \mathbf{n} is the extrinsic conormal vector of $\partial\Gamma$, given by

$$\mathbf{n} \circ \boldsymbol{\chi} \Big|_{\partial U} = \frac{n_{\beta} \mathbf{e}^{\beta}}{|n_{\beta} \mathbf{e}^{\beta}|}, \quad (\text{A.9})$$

where $|\mathbf{a}|$ denotes the Euclidean length of the vector $\mathbf{a} \in \mathbb{R}^n$. Next, let \mathbf{t} be the unit tangent vector of a 1- d curve $Y \subset \Gamma$ with conormal vector \mathbf{n} , where $Y = \boldsymbol{\chi}(Y)$ and $Y \subset U$. In local coordinates, it is given by

$$\mathbf{t} \circ \boldsymbol{\chi} \Big|_Y = \frac{t^{\alpha} \mathbf{e}_{\alpha}}{|t^{\alpha} \mathbf{e}_{\alpha}|}, \quad (\text{A.10})$$

where t^{α} is the (contravariant) tangent vector of Y . Furthermore, let $\mathbf{v} : \Gamma \rightarrow \mathbb{R}^3$ be the surface unit normal vector of Γ , which satisfies $\mathbf{n} = \mathbf{t} \times \mathbf{v}$ Walker (2015) on $\partial\Gamma$. With the ambient space \mathbb{R}^3 available, the tangent space projection $\mathbf{P} : \mathbb{R}^3 \rightarrow \mathbb{R}^3$, defined on Γ , is given by

$$\mathbf{P} = \mathbf{I} - \mathbf{v} \otimes \mathbf{v} = \mathbf{t} \otimes \mathbf{t} + \mathbf{n} \otimes \mathbf{n}, \quad (\text{A.11})$$

and note that (in local coordinates) $\mathbf{J} \mathbf{g}^{-1} \mathbf{J}^T = \mathbf{P} \circ \boldsymbol{\chi}$ Walker (2015).